Geophysical Journal International

Geophys. J. Int. (2020) **222,** 2024–2039
Advance Access publication 2020 June 05
GJI Geomagnetism, rock magnetism and palaeomagnetism

doi: 10.1093/gji/ggaa281

High-resolution palaeomagnetic record from Sea of Marmara sediments for the last 70 ka

Özlem Makaroğlu [1], Norbert R. Nowaczyk,[2] Kadir K. Eriş[3] and M. Namık Çağatay[3]

[1]*Geophysical Engineering Department, Engineering Faculty, Istanbul University-Cerrahpaşa, ,* 3432 *Avcılar, Istanbul, Turkey. E-mail: ozlemm@istanbul.edu.tr*
[2]*Helmholtz Centre Potsdam, German Research Centre for Geosciences GFZ, Section* 4.3 *– Climate Dynamics and Landscape evolution,* 14473 *Potsdam, Germany*
[3]*EMCOL Research Centre and Geological Engineering Department, Faculty of Mining, Istanbul Technical University, Ayazağa,* 34469 *İstanbul, Turkey*

Accepted 2020 June 1. Received 2020 May 23; in original form 2019 December 18

SUMMARY

Magnetostratigraphic and geochemical analyses were performed on two sediment cores recovered from the Sea of Marmara to investigate geomagnetic field variations over the last 70 ka. A chronology for each of the two cores was developed from eight AMS ^{14}C datings, tephrochronology, and tuning of Ca concentrations with stadials and interstadials observed in Greenland ice core oxygen isotope data. Based on the age models, cores MD01–2430 and MRS-CS19 reach back to 70 and 32 ka, respectively. High average sedimentation rates of 43 cm kyr^{-1} for core MD01–2430 and 68 cm kyr^{-1} for core MRS-CS19 allow high-resolution reconstruction of geomagnetic field variations for the Sea of Marmara. Mineral magnetic properties are sensitive to glacioeustatic sea level changes and palaeoclimate variations in this region, reflecting the variable palaeoenvironmental conditions of the Sea of Marmara during last 70 ka. Despite the impairment of the palaeomagnetic record in some stratigraphic intervals due to early diagenesis, relative palaeointensity variations in the Sea of Marmara sediments correlate well with similar records derived from other regions, such as the nearby Black Sea and the GLOPIS-75 stack. The directional record derived from the Sea of Marmara cores exhibits typical palaeosecular variation patterns, with directional anomalies at 41 and 18 ka, representing the Laschamps and postulated Hilina Pali excursions, respectively. Both directional anomalies are also associated with palaeointensity minima. A further palaeointensity minimum at 34.5 ka is likely related to the Mono Lake excursion, with no directional deviation documented in the Sea of Marmara palaeomagnetic record so far.

Key words: Geomagnetic excursions; Marine magnetics and palaeomagnetics; Palaeointensity; Palaeomagnetic secular variation; Palaeomagnetism.

1 INTRODUCTION

Earth's magnetic field is an important geophysical feature that is continuously recorded in rocks over geological time. Investigation of palaeomagnetic records is of profound importance in understanding the complex fluid motions within Earth's outer core. Geomagnetic palaeosecular variation (PSV) and especially excursions are associated with large-amplitude variations in the intensity of Earth's magnetic field (Panovska *et al.* 2019). These records are obtained in a large variety of archives such as lacustrine and marine sediments, lava flows, speleothems, palaeosols and archaeological remains (e.g. Kovacheva *et al.* 1998; Laj & Channell 2007; Li *et al.* 2018; Ponte *et al.* 2018; Ricci *et al.* 2018; Just *et al.* 2019). Among these archives, marine sediments have been used extensively to obtain continuous high-resolution Quaternary records of Earth's magnetic field variations (Sagnotti *et al.* 2001; Horng *et al.* 2003; Lund *et al.* 2005, 2006; Stoner *et al.* 2007; Nowaczyk *et al.* 2012; Liu *et al.* 2018, 2019; Caricchi *et al.* 2019). For example, Stoner *et al.* (2002) and Laj *et al.* (2004), using marine records with high sediment accumulation rates from different areas, provided two high-resolution palaeointensity records sapanning over the last ∼80 ka. The PISO-1500 record extending back to 1.5 Ma is also a detailed palaeomagnetic record dated using oxygen isotope chronology (Channell *et al.* 2009). These studies demonstrate that the analysed palaeomagnetic records from marine sediments are valuable for obtaining high-resolution field records and for understanding the dynamics of geomagnetic excursions for which detailed knowledge remains unknown. Although, there have been several Brunhes chron excursions (Langereis *et al.* 1997; Lund *et al.* 1998; Roberts 2008; Laj & Channell 2006, Channell *et al.* 2020), only a few such as the Laschamps and Iceland Basin excursions have been verified with precise age control (Stoner *et al.* 2003; Laj *et al.*

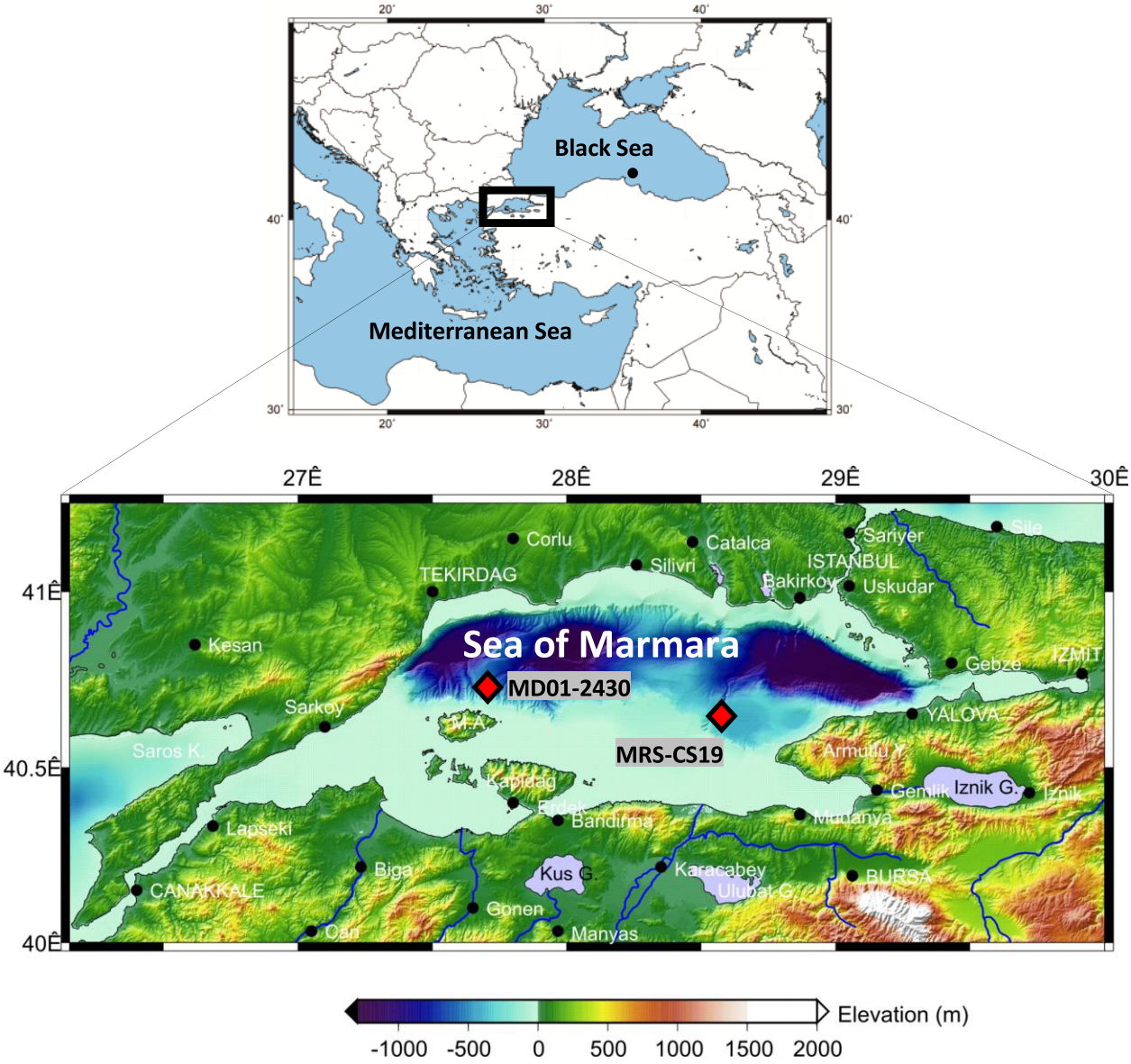

Figure 1. Study area and bathymetry of the Sea of Marmara in NW Turkey. Coring sites are indicated by red diamonds. Black dot shows the location of the core from Black Sea.

2006; Nowaczyk *et al.* 2012; Channell *et al.* 2017). Thus, continuous palaeomagnetic records from marine sediments with high-precision age control are important for understanding the excursion process. Dating of palaeomagnetic records from marine sediments can often be achieved by identifying global and regional climate proxies (e.g. Kotilainen *et al.* 2000; Nowaczyk *et al.* 2013, 2018). On a timescale from the Holocene to the Pleistocene, age models for marine sediments can be created by comparing newly obtained PSV records with master curves derived within a regional scale of several thousand kilometers. Thus, increasing the numbers of palaeomagnetic records on regional scales is crucial for understanding geomagnetic excursion dynamics and for creating reliable age models and reference records.

Many high-resolution palaeomagnetic records are available from different regions of the Earth over long timescales, including the Holocene (e.g. Thompson & Turner 1979; Lund 1996; Zheng *et al.* 2014) and the Pleistocene (e.g. Tric *et al.* 1992; Brandt *et al.* 1999; Laj *et al.* 2000; Stoner *et al.* 2002, Sagnotti *et al.* 2016). However, such records from Anatolia, are scarce. Previous studies of high-resolution palaeomagnetic records for the last 9000 yr and 350 ka from Lake Van in eastern Anatolia were performed by Makaroğlu (2011) and Vigliotti *et al.* (2014), respectively. Palaeomagnetic records from this lake have low quality due to weak natural remanent magnetization (NRM) intensities and diagenesis. Detailed palaeomagnetic studies on SE Black Sea sediments, north of Anatolia, were published by Nowaczyk *et al.* (2012, 2013, 2018) and Liu *et al.* (2018, 2019) for the last 70 ka BP. Laschamps excursion records from Black Sea sediments centered at 41 ka were presented in detail in these studies. So far, there has only been one published palaeomagnetic inclination record from the Sea of Marmara, derived from a 0.9 m core from the Western High (Fig. 1, Drab *et al.* 2015). However, this record spans only the last 2000 yr, and is affected by intense early diagenesis.

Here, we present new and well dated continuous palaeomagnetic and mineral magnetic records, together with geochemical elemental proxy data, from two long cores recovered from different

sedimentary basins in the Sea of Marmara that span the last 70 ka, comprising marine isotope stage (MIS) 1–4 (Fig. 1). We discuss the records of possible geomagnetic excursions using the well-dated cores from the Sea of Marmara. Located on the oceanographic gateway between the Black Sea and Aegean Sea, the SoM sediments constitute an important archive of palaeoclimatic and palaeoceanographic events, as well as glacioeustatic sea level changes. Hence, palaeomagnetic and mineral magnetic records from the Sea of Marmara are important for constructing coregistered temporal correlations with environmental and climatic records. Moreover, our continuous well-dated palaeomagnetic data from the Sea of Marmara provide a reference palaeomagnetic PSV record for future work in Anatolia, which includes numerous Quaternary volcanoes and archaeological sites between the two large water bodies, the Mediterranean Sea and the Black Sea.

2 REGIONAL AND OCEANOGRAPHIC SETTINGS

Several previous studies have been published on tectonics, palaeoceanographic and palaeoclimatic processes in the Sea of Marmara (e.g. Aksu *et al.* 2002; Le Pichon *et al.* 2003; Vidal *et al.* 2010, Eriş *et al*. 2007, 2008, 2011; Valsecchi *et al.* 2012; Şengör *et al.* 2014; Çağatay *et al*. 2015, 2019; Çağatay & Uçarkuş 2019). The Sea of Marmara is a small (∼210 × 75 km) intracontinental basin between the Mediterranean and Black seas. It has evolved as a series of strike-slip basins in NW Turkey (Okay *et al.* 2000; Armijo *et al.* 2002; Le Pichon *et al.* 2003; Şengör *et al*. 2005, 2014), and consists of three ∼1250-m-deep sub-basins (Çınarcık, Central and Tekirdağ) and two NE-trending Central and Western highs between the basins (Fig. 1). The northern and southern shelves, which border the deep basins, have a shelf break at 90–100 m water depth. Other notable morphological features of the Sea of Marmara include the ∼400-m-deep İmralı Basin between the Çınarcık Basin and southern shelf and E–W extending gulfs of İzmit and Gemlik in the east. The main sediment and fresh water inputs in the Sea of Marmara occur from the south, where the largest catchment area with relatively large rivers (Susurluk-Kocasu and Gönene rivers) is located (EİE 1993; Okay & Ergün 2005).

The straits of the Dardanelles (Çanakkale) and Bosphorus (İstanbul) connect the Sea of Marmara to the Aegean Sea and the Black Sea, having present-day sill depths of −65 and −35 m, respectively (Çağatay *et al.* 2015). Two-way water exchange occurs via both straits and the Sea of Marmara between the Mediterranean and Black Sea waters with salinities of 38 and 18 ‰, respectively. A permanent pycnocline is present at −25 m between the two water masses (Ünlüata *et al.* 1990; Beşiktepe *et al.* 1994; Chiggiato *et al.* 2012). Due to shallow sill depths of its connecting straits, however, the Sea of Marmara lost its connection with neighbouring seas during glacial sea level lowstands (Çağatay *et al*. 2009, 2019; Eriş *et al.* 2011), and its water level changed independently of the global sea level.

Its oceanographic setting, as a gateway between the Black and Aegean seas, makes the Sea of Marmara sediments an important palaeoceanographic and palaeoclimatic archive. As a result, considerable work has been carried out on the late Pleistocene to Holocene palaeoceanography and palaeoclimatology of the Sea of Marmara (e.g. Aksu *et al.* 2002; Eriş *et al.* 2007; McHugh *et al.* 2008; Çağatay *et al*. 2009, 2015; Vidal *et al.* 2010; Valsecchi *et al.* 2012). A ∼29 m giant piston core (MD01–2430) from the Western High contains two main sedimentary units (i.e. an upper marine and a lower lacustrine units) and extends back to 67 cal ka BP: (Çağatay *et al.* 2015). This record, therefore, indicates that the Sea of Marmara separated from the Aegean Sea from the beginning of MIS 4 to the end of MIS 2. During this period, sea level was below the sill depth of Çanakkale Strait (Çağatay *et al.* 2009; Eriş *et al.* 2011), and the Sea of Marmara was a fresh to brackish lake. Therefore, during this period the water level of the Marmara 'Lake' was only controlled by fresh water input from the Black Sea and the sill depth of the Çanakkale Strait (Çağatay *et al.* 2015). Greenland Interstadial (GI) periods during MIS 4–3 in the Sea of Marmara are characterized by relatively higher organic productivity, higher endogenic carbonate deposition, and lower detrital input relative to stadial periods (Çağatay *et al.* 2015). The entire lacustrine unit of MIS 4–2 was deposited under oxic water conditions (Çağatay *et al.* 2015).

Çağatay *et al.* (2015) found that the latest marine reconnection of the Sea of Marmara to Mediterranean Sea was at 12.6 cal ka but that the initial marine connection was somewhat earlier, at ∼14.7 cal ka according to the $^{87}Sr/^{86}Sr$ isotope ratio of ostracod shells in the same core (Vidal *et al.* 2010). Full marine connection was established, and then a lower Holocene sapropel was deposited in the Sea of Marmara under suboxic–anoxic conditions during 12.3–5.7 cal. ka interval (Tolun *et al.* 2002; Çağatay *et al*. 2009, 2015).

3 MATERIAL AND METHODS

3.1 Core recovery and palaeomagnetic sampling

The studied cores, MD01–2430 (40.7968°N/27.7253°E) and MRS-CS19 (40.6295°N/28.8527°E), were recovered from the Western High by RV *Marion Dufresne* in 2001 and from east of the İmralı Basin by RV *Pourquoi pas?* in 2014, respectively (Fig. 1, Table 1). Core MD01–2430 was sampled in the *Laboratoire des Sciences du Climat et de l'Environnement* (LSCE), Gif-sur-Yvette, France in 2017. It was previously studied in detail for lithological and geochemical analyses by Çağatay *et al.* (2015). Splitting and sampling of core MRS-CS19 was done at the Palaeomagnetic Laboratory in Istanbul University-Cerrahpaşa. Lithological descriptions and geochemical measurements were performed at the Istanbul Technical University, Eastern Mediterranean Centre for Oceanography and Limnology (ITU-EMCOL). The working halves of core MRS-CS19 were sampled for palaeomagnetic and radiocarbon analyses. Archive core halves were analysed for elemental μ-XRF analysis at ITU-EMCOL.

3.2 Age dating and tuning procedure

The chronology of the two cores is based on radiocarbon analysis (accelerator mass spectrometry; AMS), tephrochronology and correlation with Greenland ice core stable isotope data. AMS ^{14}C dates from marine mollusc shells were used to establish the age–depth model of core MRS-CS19. Calendar ages were determined by using the INTCAL13 (Reimer *et al.* 2013) calibration curve. One tephra layer in core MRS-CS19 was correlated with the Santorini tephra (Cape Riva), which has an age of 22 ka (Pichler & Friedrich 1976; Eriksen *et al.* 1990; Druitt *et al.* 1999; Fabbro *et al.* 2013). This ash layer was previously found in cores from the Sea of Marmara by Wulf *et al.* (2002) and Çağatay *et al.* (2015, Table 2). Core MD01–2430 was dated previously by Çağatay *et al.* (2015) using five AMS ^{14}C dates from Vidal *et al.* (2010), tephrochronology (Table 2), and age tie-points obtained by tuning of the core's Ca-record to the onset of GIs observed in the NGRIP $\delta^{18}O$ record

Table 1. Details for the studied cores in the Sea of Marmara.

Core name	Location	Water depth (mbsl)	Core length (cm)	Tephra	Number of palaeomagnetic samples
MD2430	40.7968°N 27.7253°E	580	2888	Avellino (161 cmbsf)	1042
				Cape Riva (698 cmbsf)	
				Campanian Ignimbrite (1520 cmbsf)	
MRS-CS19	40.6295°N 28.8517°E	365	2264	Cape Riva (1800 cm)	882

Table 2. AMS radiocarbon dates and tephra ages.

Core	Dating material	Depth in core (cm)	Cal. AMS ^{14}C (ka)	Reference
MD01–2430	Proximal tephra **(Avellino; Av)**	161	3.96 ± 10	Hammer *et al.* 1987; Sevink *et al.* 2011
MD01–2430	Proximal tephra, **(Cape Riva; Y-2)**	698	22.0 + 854/−902	Pichler & Friedrich 1976; Eriksen *et al.* 1990; Druitt *et al.* 1999; Roeser *et al.* 2012; Fabbro *et al.* 2013
MD01–2430	Proximal tephra, **(Campanian Ignigbride (CI/Y-5)**	1520	39.28	Fisher *et al.* 1993; De Vivo *et al.* 2001; Giaccio *et al.* 2017
MRS-CS-19	Bivalve shell	303	3.26 ± 51	This study
MRS-CS-19	Bivalve shell	763	7.73 ± 70	This study
MRS-CS-19	Bivalve shell	863	8.43 ± 43	This study
MRS-CS-19	Proximal tephra **(Cape Riva; Y-2)**	1800	22.0 + 854/−902	Pichler & Friedrich 1976; Eriksen *et al.* 1990; Druitt *et al.* 1999; Roeser *et al.* 2012; Fabbro *et al.* 2013

(Andersen *et al.* 2006; Svensson *et al*. 2006, 2008; Wolff *et al.* 2010).

In this study, our palaeomagnetic data sets (relative palaeointensity and inclination) over the last 70 ka were correlated simultaneously in detail to the Black Sea palaeomagnetic stack (Nowaczyk *et al.* 2013; Liu *et al.* subm.), while geochemical records (XRF-Ca counts) and low-field magnetic susceptibility (κ_{LF}) were tuned to the δ^{18}O record from the North Greenland Ice Core Project (NGRIP members 2004; Svensson *et al*. 2006, 2008). Tuning was performed using software, extended tool for correlation (xtc), developed at the Helmholtz-Centre Potsdam (GFZ), Germany.

3.3 Geochemical analysis

An ITRAX μ-XRF (X-ray fluorescence) core scanner equipped with XRF-EDS was used to analyse multi-element analysis of core MRS-CS19 at 0.5 mm resolution (Croudace *et al.* 2006; Thomson *et al.* 2006). Relative elemental concentrations were recorded as counts per second (cps).

3.4 Palaeomagnetic analyses

For standard palaeo- and mineral magnetic analyses, a total of 1924 oriented samples along the *z*-axes of the cores were taken from cores MD01–2430 and MRS-CS19 using plastic boxes with 6.0 cm^3 volume. The analyses included κ_{LF} measurements, NRM, anhysteretic remanent magnetization (ARM), and isothermal remanent magnetization (IRM). All analyses were performed on all discrete samples at the Laboratory for Palaeo- and Rock Magnetism at the GFZ Potsdam, Germany. First, a Multifunction Kappabridge susceptibility meter (MFK-1S) was used to measure κ_{LF}. Then, NRM and ARM vectors were measured and demagnetized using a 2-G Enterprises cryogenic (755-SRM long-core) magnetometer, while IRM vectors were measured with a Molyneux spinner magnetometer. Stepwise demagnetization of the NRM was performed with an alternating field (AF) demagnetizer in ten steps from 5 to 100 mT to identify the NRM directions and to remove the secondary magnetizations. To calculate relative palaeointensity (rPI) variations using ARM normalization, ARM was acquired with a 2-G Enterprises demagnetizer with ARM coil using 100 mT AF and 0.05 mT static field. Principal component analysis (Kirschvink 1980) was used to determine characteristic remanent magnetization (ChRM) inclinations and declinations, with demagnetization data not anchored to the origin. The median destructive field (MDF) of the ARM was determined from stepwise demagnetization at seven AF steps from 0 to 65 mT. Relative palaeointensity (rPI) was estimated from the slope of NRM versus ARM demagnetization steps, generally from 20 to 50 mT for the application of linear regression because here the trend was mostly linear with intercept values around zero. Choosing this interval ensures that the same portions of the coercivity spectrum from both the NRM and the ARM intensities are providing to the estimate of rPI. (e.g. Levi & Banerjee 1976; Tauxe 1993; Valet 2003).

The saturation IRM (SIRM) was acquired in a maximum field of 1.5 T. A reversed field of −0.2 T, by laboratory experience the optimum field to separate magnetite from haematite, was used remagnetize the samples ($IRM_{-0.2T}$) in order to determine the *S*-ratio, which is defined as: *S*-ratio = 0.5 × [1 − ($IRM_{-0.2T}$/SIRM)] (after

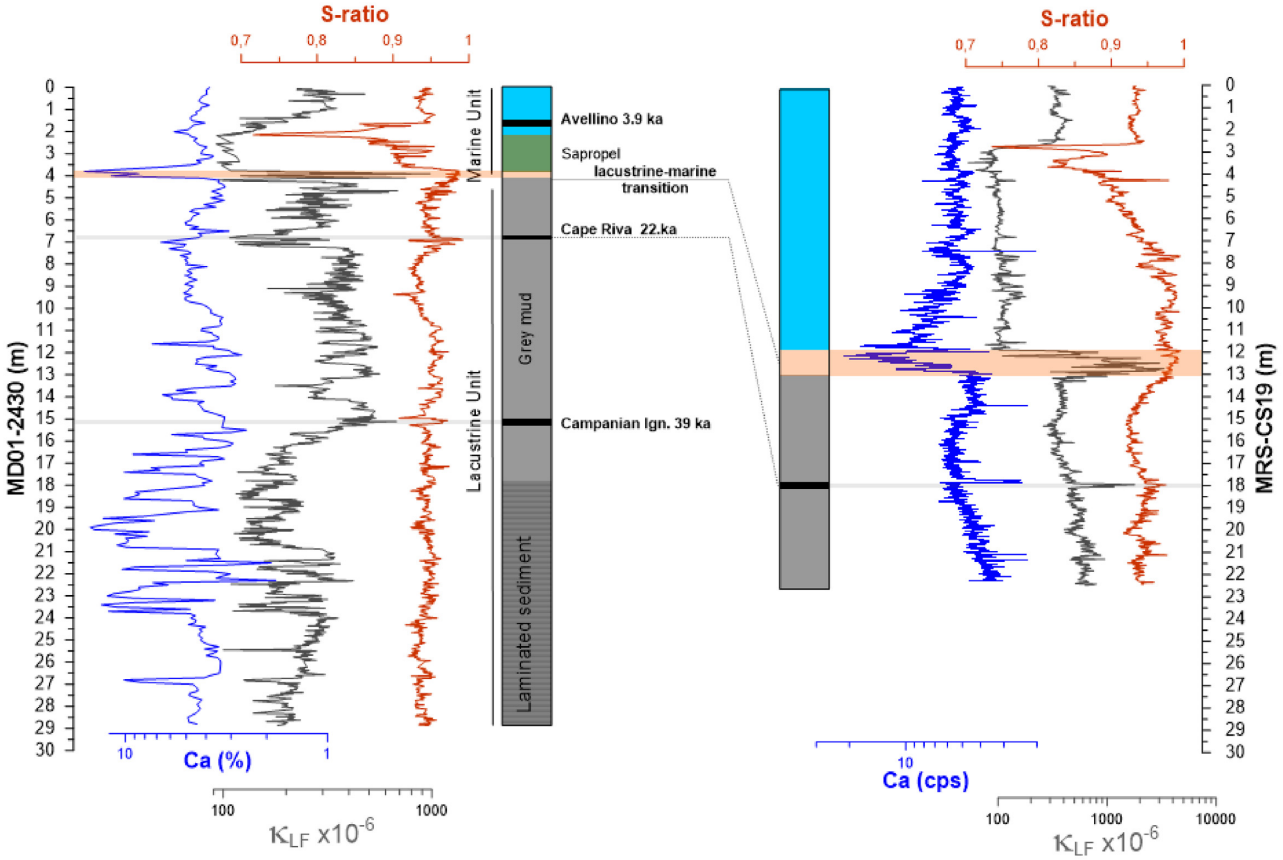

Figure 2. Simplified lithology, down-core magnetic susceptibility (κ_{LF}), *S*-ratio and Ca (μ-XRF-count per second; cps) profiles for cores MD01–2430 and MRS-CS19. Orange bars represent the lacustrine-marine transition. Black and grey bars mark tephra layers and dashed lines indicate main correlative depths between the cores. The cores include marine and lacustrine units in blue and grey, respectively. The marine unit of MD01–2430 includes one sapropel layer (green).

Bloemendal *et al.* 1992). If the samples are dominated by high-coercivity minerals (e.g. haematite and goethite), the *S*-ratio value is close to 0, whereas samples dominated by low coercivity minerals (e.g. magnetite and greigite) will have values close to 1. Greigite-bearing samples are indicated by SIRM/κ_{LF} values higher than 10 kAm^{-1}. High SIRM/κ_{LF} values obtained from marine sediments clearly indicate significant amount of secondary magnetizations as shown by many studies (e.g. Snowball & Thompson 1990; Snowball 1991; Roberts & Turner 1993; Reynolds *et al.* 1994; Ron *et al.* 2007; Nowaczyk *et al.* 2012). Thus, such samples are assumed to have a secondary magnetization and were removed from the palaeomagnetic record.

4 RESULTS

4.1 Sedimentology and chronology

The studied cores (MD01–2430 and MRS-CS19) consist essentially of an upper marine unit and a lower lacustrine unit (Fig. 2). The lacustrine–marine (L/M) transition and some levels of the lacustrine unit in both cores are characterized by the presence of black greigite, which rapidly oxidizes to rusty brown colours upon exposure of the core surface to atmosphere.

The lithology, geochemistry, and chronology of core MD-2430 was previously documented in detail by Çağatay *et al.* (2015), whereas core MRS-CS19 is examined for the first time in this study. Core MD01–2430 comprises a marine unit with a sapropel layer in the upper 3.8 m. This unit contains euryhaline marine bivalves and microfossils, whereas the lacustrine unit is characterized by homogeneous and laminated mud between 3.8 and 18 m below sea floor (mbsf) with alternations of carbonate- and clay-rich bands in the lower 10.9 m of the core (Çağatay *et al.* 2015). Three distinct tephra layers are present in core MD01–2430. Starting from oldest to youngest, these are the 'Campanian Ignimbrite', or Y-5 tephra (39.3 ka, e.g. Fisher *et al.* 1993; De Vivo *et al.* 2001; Giaccio *et al.* 2017), the Santorini 'Cape Riva' (Y-2) tephra (22.0 ka; e.g. Fabbro *et al.* 2013), and the 'Avellino' tephra (3.96 ka, e.g. Hammer *et al.* 1987; Sevink *et al.* 2011, Fig. 2; Tables 1 and 2).

In core MRS-CS19, the L/M transition is documented at 13.05 mbsf, and the Santorini 'Cape Riva' tephra is found at 18.0 mbsf in the lacustrine unit that consists of olive-gray homogeneous clay. Three AMS radiocarbon datings were obtained from bivalve shells in the marine part of the core (Table 2). Additional age tie-points (Fig. 4) were obtained by tuning Ca data (counts) to the δ^{18}O record from the NGRIP ice core (Fig. 3). The rationale behind this tuning is that positive Ca excursions in the siliciclastic lacustrine unit of MIS 2–4 in the Sea of Marmara and Black Sea (Nowaczyk *et al.* 2012; Çağatay *et al.* 2015) have lower amplitude magnetic susceptibility variations because of dilution by diamagnetic carbonates. Therefore, the magnetic susceptibility and Ca counts of the cores are (anti-)correlated with the δ^{18}O of the NGRIP record.

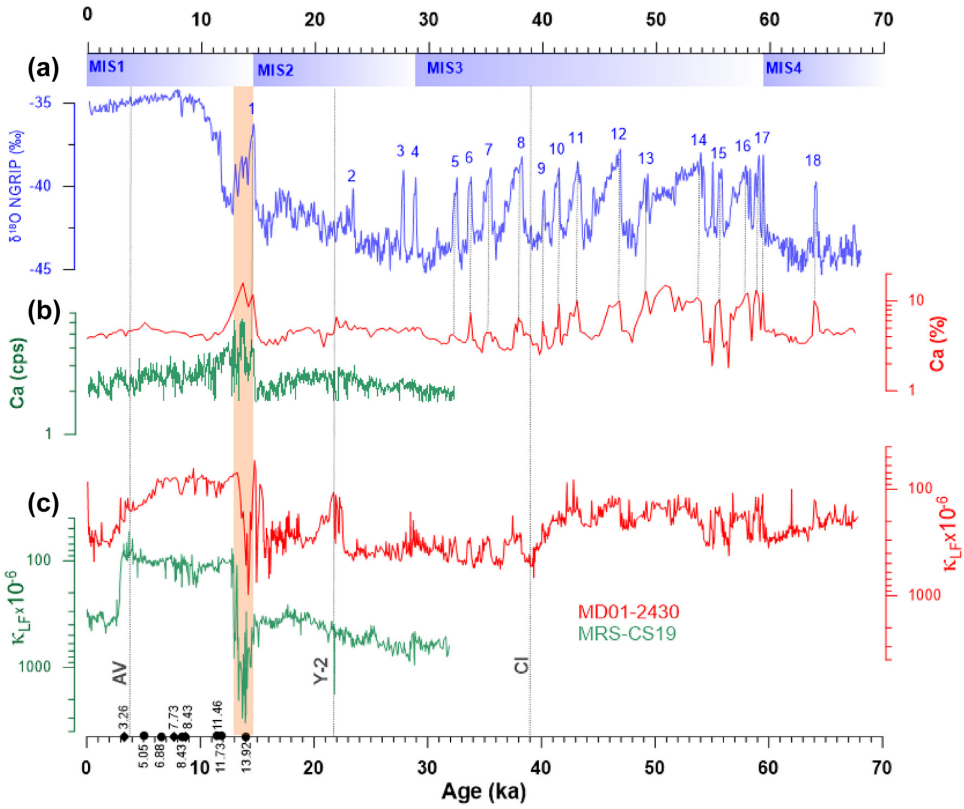

Figure 3. Magnetic susceptibility (κ_{LF}) and Ca (μ-XRF-count per second; cps) for cores MRS-CS19 and MD01–2430 from the Sea of Marmara tuned to $\delta^{18}O$ data from the NGRIP over the last 70 ka. (a) Greenland NGRIP ice core $\delta^{18}O$ record (GIC05 time scale) (Svensson *et al*. 2006, 2008) and MIS boundaries (blue bars). Numbers in the NGRIP plot indicate Dansgaard-Oescher warming events (Dansgaard *et al.* 1993; Svensson *et al*. 2006, 2008; Rasmussen *et al.* 2006; Wolff *et al.* 2010); (b) XRF Ca records from cores MD01–2430 (Çağatay *et al.* 2015) and MRS-CS19 (this study); (c) magnetic susceptibility data after simultaneous tuning to the $\delta^{18}O$ record in (a). Dashed vertical lines mark the stratigraphic positions of tephra layers AV (Avellino), Y-2 (Cape Riva), CI (Campanian Ignimbrite, Y-5) and correlation point between Ca and NGRIP record. Diamont and circles show radiocarbon ages of MRS-CS19 and MD01–2430, respectively. The orange vertical bar marks the lacustrine-marine transition zone.

According to our age models, cores MD01–2430 and MRS-CS19 cover the last 70 and 32 ka, respectively (Fig. 4) with continuous deposition at average sedimentation rates of ∼43 and 68 cm kyr^{-1}, respectively (Fig. 4). Such high sedimentation rates without a sedimentary hiatus enables development of a continuous high-resolution palaeomagnetic records from the Sea of Marmara.

4.2 Mineral magnetic properties

Down-core variations of magnetic properties, NRM and ARM intensities (concentration), κ_{ARM}/κ_{LF} (grain size), *S*-ratio (mineralogy) and SIRM/κ_{LF} (mineralogy, grain size) are shown in Fig. 5. Detrital magnetic minerals dominate the Sea of Marmara sediments. The presence of secondary diagenetic iron sulphide mineral (e.g. greigite) in the L–M transition zone and parts of laminated Pleistocene lacustrine unit is evidenced by a high SIRM/κ_{LF} ratio between 15 and 100 kAm^{-1} (Fig. 5). Such high values are considered to be indicative of the secondary magnetic iron sulphide minerals also by previous studies (e.g. Snowball 1991; Roberts & Turner 1993; Nowaczyk *et al*. 2012, 2013). High *S*-ratio values for most of the samples suggest the predominance of low coercivity minerals, that is, mainly magnetite, with some greigite (Fig. 5).

4.3 Palaeo- and rock magnetism

Down-core plots of palaeomagnetic results from the two studied cores, including ChRM inclination and declination, rPI, the median destructive field of the NRM (MDF_{NRM}), and maximum angular deviation (MAD) for ChRM fits, are shown in Fig. 6. NRM intensities range between 0.1 and 60 mAm^{-1} in core MD01–2430 and between 0.2 and 420 mAm^{-1} in core MRS-CS19, respectively. Values of both MDF_{NRM} and MAD increase toward the bottom of the core. In particular, a marked step occurs at around 16 m (∼40 ka BP) in core MD01–2430 with average MAD values of 3.0° above and 7.2° below this level (Fig. 6). This change occurs in the lacustrine unit, close to the transition from the laminated and banded mud below to the homogeneous lacustrine mud above. High MAD values >5° generally indicate a relatively low magnetic mineral concentration and low detrital input, or post-depositional dissolution. In both cores MAD values are frequently <5° (77 per cent of the data), which indicates stable ChRM directions for the studied Sea of Marmara cores (Fig. 6).

For the study area the inclination expected for a geocentric axial dipole (GAD) is 60°. The mean inclination (50°) for the cores is less than this value, which indicates some degree of inclination shallowing. Overall, directional data from the two studied cores have typical PSV patterns, although with noise in intervals with high MAD values (Fig. 6).

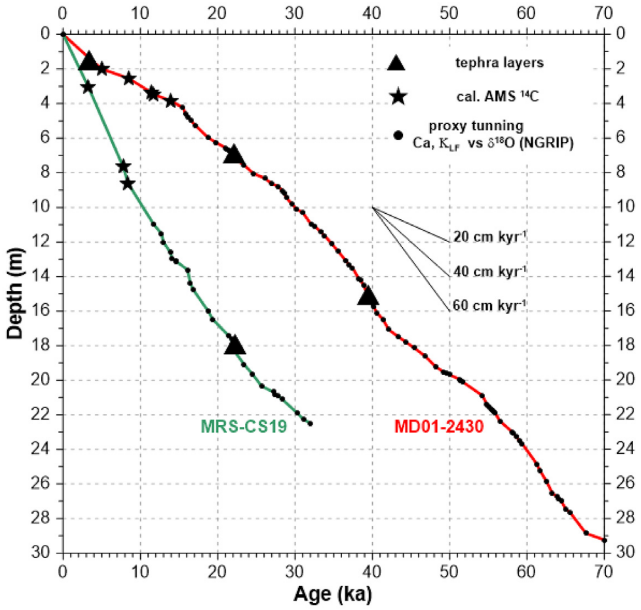

Figure 4. Age–depth model for cores MD01–2430 and MRS-CS19 from the Sea of Marmara created using calibrated AMS ^{14}C ages (stars) and multiparameter tuning to the NGRIP ice core record (Svensson *et al*. 2006, 2008) and published ages of tephras, Avellino (AV) (Hammer *et al.* 1987; Sevink *et al.* 2011), Cape Riva (Y-2) (Pichler & Friedrich 1976; Eriksen *et al.* 1990; Druitt *et al.* 1999; Roeser *et al.* 2012; Fabbro *et al.* 2013) and Campanian Ignimbrite tephra (CI/Y-5) (Fisher *et al.* 1993; De Vivo *et al.* 2001; Giaccio *et al.* 2017). Radiocarbon dates and tephra ages were used as initial tie points for the age models. XRF Ca and κ_{LF} features (solid dots) were than correlated between those age tie points to the NGRIP δ^{18}O record.

In core MD01–2430, from the core top to ∼8 mbsf, including the marine unit with the sapropel layer, two tephra layers and the L–M transition, are characterized by noisy and unstable palaeomagnetic results, whereas in the interval between 8 and ∼17.15 mbsf palaeomagnetic data are more stable. Below ∼17.15 mbsf there is a clear shift to shallower and noisier inclinations (Fig. 6). This lower part of the core MD01–2430 succession consists of laminated sediments, likely indicating sulphidisation of detrital iron oxides, including magnetite. Therefore, this part was omitted from our palaeomagnetic interpretation. The depth interval from 16.50 to 16.55 mbsf, corresponding to 41 ka BP, is characterized by a sharp inclination swing to values around −50° and a clear palaeointensity decrease (Fig. 6). AF demagnetization results from Core MD01–2430, plotted as Zijderveld diagrams (Zijderveld 1967), show that samples between 16.45 and 16.24 mbsf interval all have upward directed vectors (Fig. 7). However, declinations within this interval are westerly, but not southerly oriented. Thus, the directions are 'transitional' rather than 'reversed'. For comparison, a clear normal polarity sample from 0.10 m below the excursion, with a northward declination and a steep downward inclination, is shown in Fig. 7(f).

Inclinations in Holocene sediments in core MRS-CS19 are close to the expected GAD value (Fig. 6). Palaeomagnetic directions in core MRS-CS19 are generally more stable than those in core MD01–2430. Between 15.51 and 17.60 mbsf in core MRS-CS19 shallow (partly negative) inclinations are recorded (Fig. 6).

5 DISCUSSION

5.1 Diagenetic effects in the Sea of Marmara sediments

Core MRS-CS19, located in İmralı Basin, has higher sedimentation rates than MD01–2430, and provides a relatively more stable and reliable high-resolution palaeomagnetic record than core MD01–2430. This difference in the quality of records is related to the rates of early diagenetic reactions in the anoxic zone (i.e. sulphate reduction, methanogenesis and anaerobic oxidation of methane), which are controlled by the amount of metabolizable organic matter, sedimentation rate (i.e. rate of detrtital influx), 'reactive' iron (ferrihydrite, lepidocrocite, goethite and haematite) and rate of upward methane flux at the coring sites (Froelich *et al.* 1979; Borowski *et al.* 1996; Çagatay *et al*. 2001, 2004; Roberts 2015). These controlling factors also determine the depth and thicknesses of the various diagenetic zones. In particular, sedimentation rate affects diagenesis by exerting a control on the burial rate of organic carbon and the upward and lateral advection of pore water and its dissolved constituents (e.g. Muller & Suess 1979; Morse & Mackenzie 1990; Çağatay *et al.* 2001; Roberts 2015). In rapidly accumulating sediments, pore waters can be advected toward the seafloor, resulting in a low downward diffusion of seawater constituents (e.g. sulphate) into the sediments. Reactive iron oxides in subsurface sediments, provided mainly by riverine and wind transportation, are important oxidants in suboxic diagenetic reactions and are significant in determining sulfate reduction rates (e.g. Froelich *et al.* 1979; Berner 1980). Sediments with a high content of reactive iron have thicker suboxic zones, thinner sulfate reduction zones and deeper sulphate–methane interface (SMI) than those in the reactive-iron limited sediments (Raiswell & Berner 1985; Canfield 1989; Schulz 2000; Fossing & Jørgensen 1990; Çağatay *et al.* 2001).

We conclude that core MRS-CS19, with its location close to the riverine sediment source, and hence, its high sedimentation rates (68 cm kyr^{-1}) with high detrital siliciclastic and iron oxide inputs, would be expected to be less affected by early diagenetic processes than core MD01–2430, which is from the Western High and has lower average sedimentation rate (43 cm/kyr). This conclusion is supported by previous studies in the Sea of Marmara, which indicate that the SMI occurs in locations variable in different morphological parts of the Sea of Marmara: the SMI is located at depths of 4.0–4.5 mbsf on the western high (Halbach *et al.* 2004; Tryon *et al.* 2010), at 3.4 mbsf in Çınarcık Basin and at 2.4 mbsf over the southern shelf (Çağatay *et al.* 2004).

5.2 Quality of the palaeomagnetic records and its relation to palaeoevironmental conditions

Although the laminated and banded lower part of the lacustrine unit below 17.15 mbsf in core MD01–2430 has a poor palaeomagnetic record, the dark grey homogenous mud interval at 3.80–17.15 mbsf (corresponding to 12–43 ka) has fairly stable and well defined magnetization directions (Figs 2, 6 and 8). Unstable palaeomagnetic results from the lower laminated and banded lacustrine unit coincide with relatively high Ca and TOC contents (Çağatay *et al.* 2015). These, together with the presence of laminations, suggest relatively high organic productivity and suboxic to anoxic bottom-water conditions suitable for organic matter burial but unfavorable for magnetic mineral preservation (Nowaczyk *et al.* 2002). Therefore, we consider the interval between about 70 and 50 ka from core MD01–2430 as unsuitable for palaeomagnetic studies (Figs 6 and 8). Core MRS-CS19 does not reach the laminated and banded

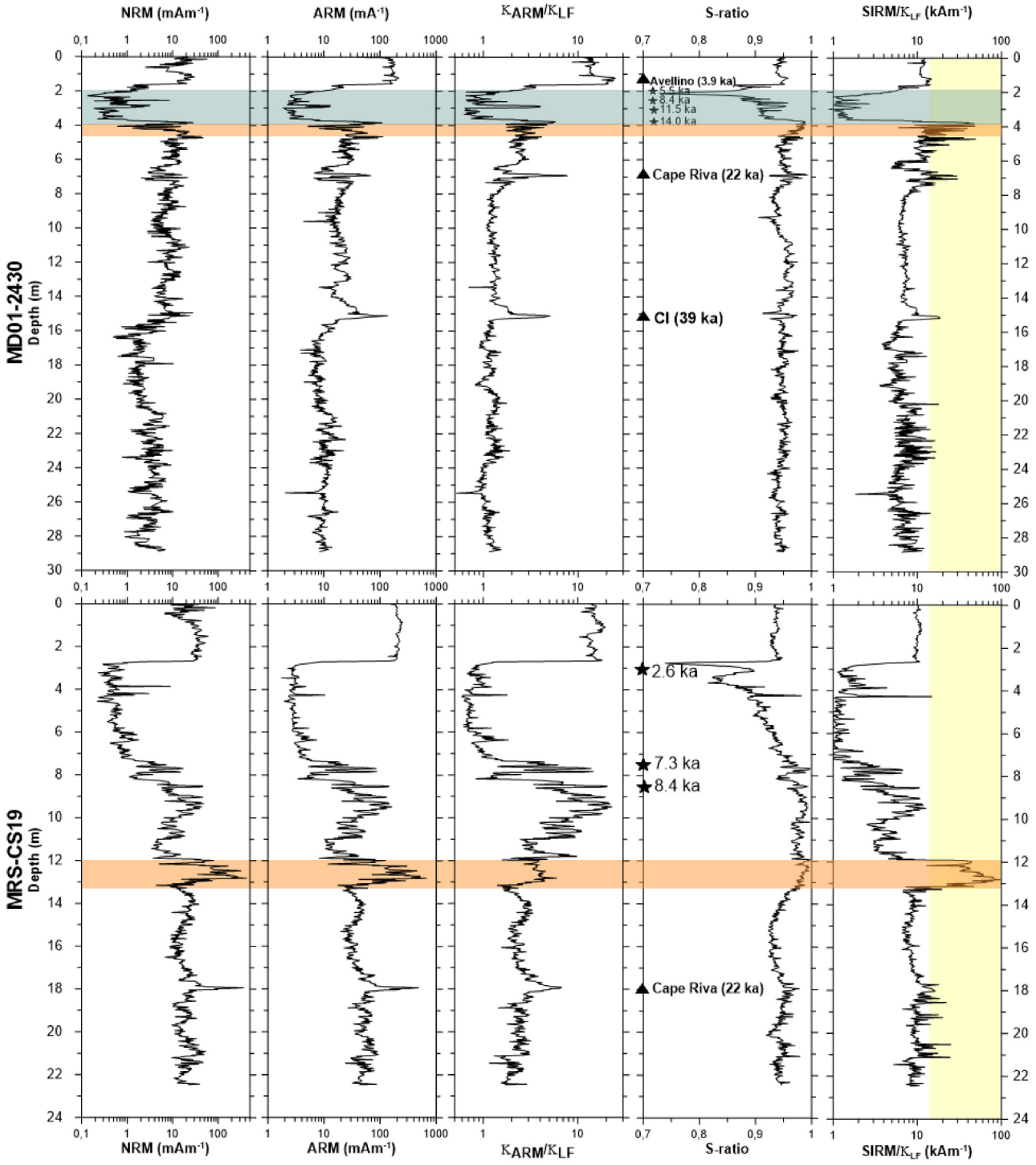

Figure 5. Down-core variations of magnetic mineral concentration (NRM, ARM), grain size (κ_{ARM}/κ_{LF}), and magnetic mineralogy (*S*-ratio, SIRM/κ_{LF}) from cores MD01–2430 and MRS-CS19. Yellow bar indicates secondary magnetic iron sulphide. The orange bar marks lacustrine to marine transition; the green bar indicates a sapropel layer in core MD01–2430. Stars denote AMS ^{14}C dates, triangles: tephra layers.

sediment interval of MIS 3 and 4, thus prohibiting comparison between magnetic records of the two cores for that interval.

Low values of κ_{LF} (Fig. 2), *S*-ratio and SIRM/κ_{LF} over the last *ca*. 15 ka BP correspond to changes in sediment lithology and geochemistry, associated mainly with sea level rise and marine transgression into the Sea of Marmara at 14.7 ka BP (Vidal *et al.* 2010; Eriş *et al.* 2011). This initial transgression was followed by sapropel deposition under suboxic-anoxic conditions in the Sea of Marmara (Tolun *et al.* 2002; Çağatay *et al.* 2015). Arrival of sulphate-rich marine waters intiated more vigorous bacterial sulphate reduction in the lacustrine-marine transition zone and in the marine sequence of the Sea of Marmara. This is clearly seen in core MD01–2430 from the

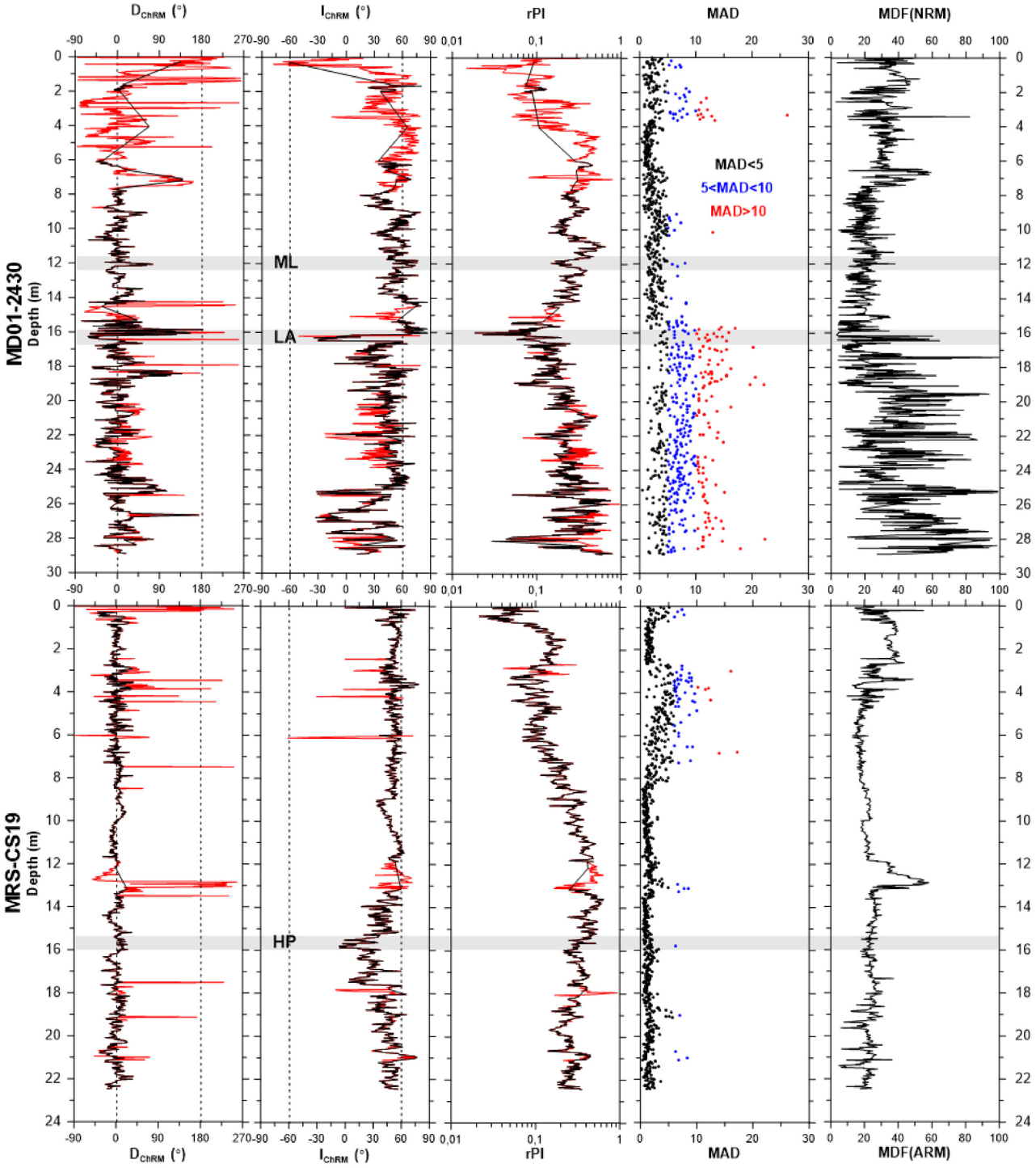

Figure 6. Down-core variations of palaeomagnetic data from cores MD01–2430 and MRS-CS19. Red curves for ChRM declination (D_{ChRM}), ChRM inclination (I_{ChRM}) and relative palaeointensity (rPI), derived from the slope of NRM versus ARM, represent complete (raw) data sets, whereas black curves represent final data sets filtered from the effects of greigite indicated by the grey area in Fig. 5 (outer right). MAD = maximum angular deviation, MDF = median destructive field, ARM = anhysteretic remanent magnetization. ChRM = characteristic remanent magnetisation. The inclination (±60°) and declination (0, 180°), as expected for a geocentric axial dipole are shown by the vertical dashed lines in the directional plots.

Western High, which has a noisy palaeomagnetic record and low palaeointensity estimates throughout the Holocene (Figs 6 and 8). Drab *et al.* (2015) also reported that a palaeomagnetic record for the last 2 ka from the Western High is affected strongly by reductive diagenesis.

The high sedimentation rates (>35 cm kyr^{-1}) in the studied cores result from fluvial input and the semi-isolated nature of the the Sea of Marmara basin, and allows the study of high resolution excursion records from the basin. Such rates above 10 cm kyr^{-1} in marine sediments are considered acceptable to obtain meaningful

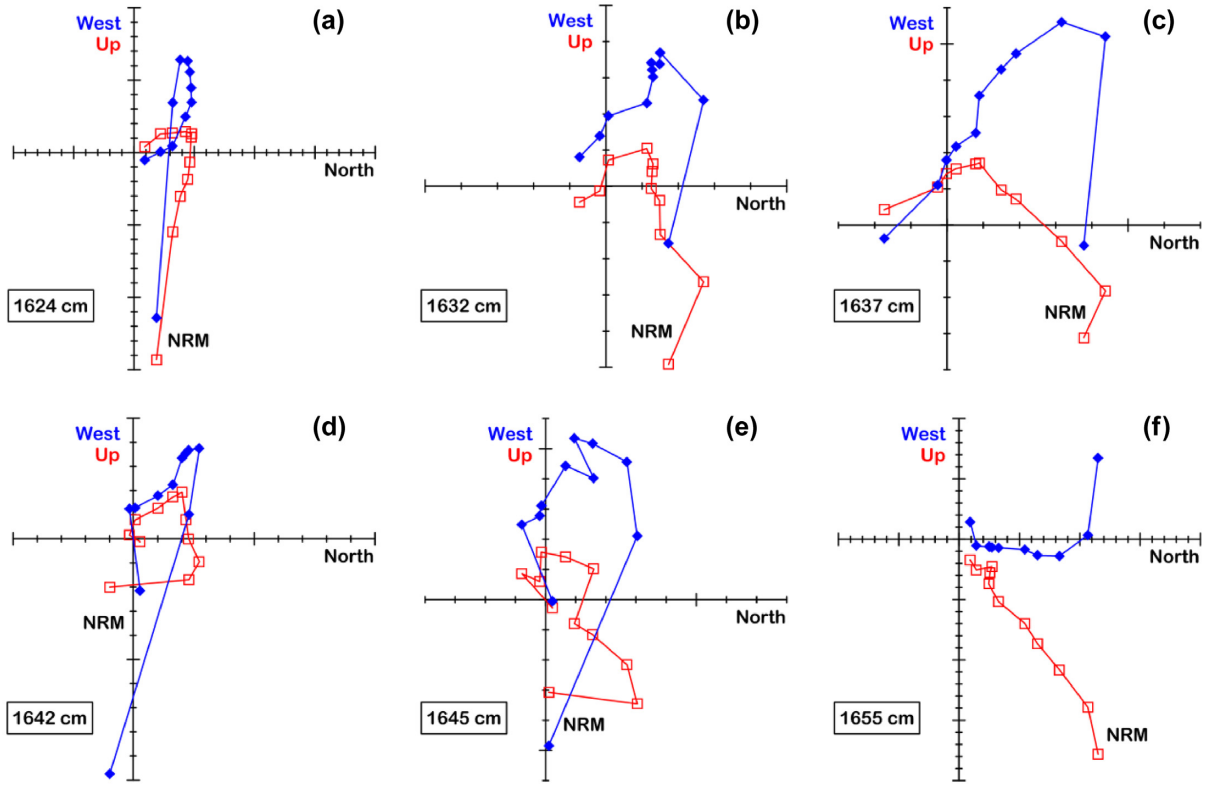

Figure 7. AF demagnetization results from selected samples along the Laschamps excursion as recorded in Core MD01–2430, displayed as Zijderveld diagrams. Closed blue diamonds mark variations in the horizontal plane (W versus N) and open red squares mark variations in the vertical plane (Z versus N). Samples from (a) through (e) have upward directed vectors during the Laschamps excursion (~41 ka), whereas the sample in (f) has clear normal polarity some hundred years before the excursion. The distance between two long ticks are equal to 0.5 mA m^{-1}.

vector records of geomagnetic field behavior (Roberts & Winklhofer 2004).

5.3 Relative palaeointensity records and geomagnetic excursions

The Sea of Marmara rPI variations obtained from the slope of NRM/ARM are compared in Fig. 8 with rPI data from GLOPIS-75 (Laj *et al.* 2004) and the Black Sea palaeomagnetic stack (Liu *et al.* subm.). Both the rPI and inclination records from the Sea of Marmara and Black Sea match well between 50 and 15 ka BP. The Sea of Marmara rPI record is also in general agreement with GLOPIS-75 (Laj *et al.* 2004, Fig. 8).

The lowest rPI values in the Sea of Marmara record occur at 41 ka, and are accompanied by transitional inclinations. Thus, we interpret this feature in the Sea of Marmara palaeomagnetic record as the Laschamps excursion, which was followed by the Campanian Ignimbrite eruption in the Gulf of Naples at 39.3 ka (De Vivo *et al.* 2001, CI in Fig. 8). The Laschamps event was a brief episode with a short but full reversal of the geomagnetic field at around 41 ka. This short reversal was accompanied by a drop in field intensity (Bonhommet & Zähringer 1969; Thouveny *et al.* 1994; Laj *et al.* 2000, 2006; Lund *et al.* 2005; Nowaczyk *et al.* 2012, 2013).

Low palaeointensity values and fully reversed polarity directions are typical of the Laschamps excursion (Bonhommet & Babkine 1967; Gillot *et al.* 1979; Roperch *et al.* 1988; Chauvin *et al.* 1989; Guillou *et al.* 2004; Plenier *et al.* 2007). Since the discovery of the Laschamps excursion in the late 1960 s many further studies from globally distributed sites have proven its occurrence (e.g. Laj *et al.* 2000; Nowaczyk *et al.* 2003; Lund *et al.* 2005, 2006; Channell 2006; Channell *et al.* 2012; Laj & Channell 2015; Li *et al.* 2018).

The Black Sea palaeomagnetic record is the only study to provide clear evidence for the Laschamps excursion as a full reversal in SE Europe/West Asia (Nowacyzk *et al.* 2012). Compared to this finding, the palaeomagnetic record from core MD01–2430 in the Sea of Marmara is less well developed because it is only recorded by a few samples with upward inclinations and westerly, instead of southerly directions. This record of the Laschamps excursion in core MD01–2430 is probably affected by core disturbance and storage effects (some drying) by frequent previous sampling for different analyses and lon-term storage between its recovery in 2001 and our sampling in 2017. Directional palaeomagnetic record are known to have been effected by such factors (Verosub 1977; Verosub & Banerjee 1977; Roberts & Winklhofer 2004). Any change in the size, composition, position or relative abundance of the magnetic carriers during storage and sampling can affect directly the intensity of the magnetization (Verosub 1977). Slumped or deformed material can acquire a post disturbance magnetization. Sediments which consist of mixture of spherical particles and disc-shaped particles whose magnetic moment is the plane of the disc (Verosub 1977). These particles normally remain aligned with the earth's magnetic field when they deposited. During the storage and previous sampling the alignment of these particles could be disturbed. Viscous remanent magnetizations is also affected by the storage and handling history of a core as well as its physical state (Verosub & Banerjee 1977). Recording of directional geomagnetic field anomalies

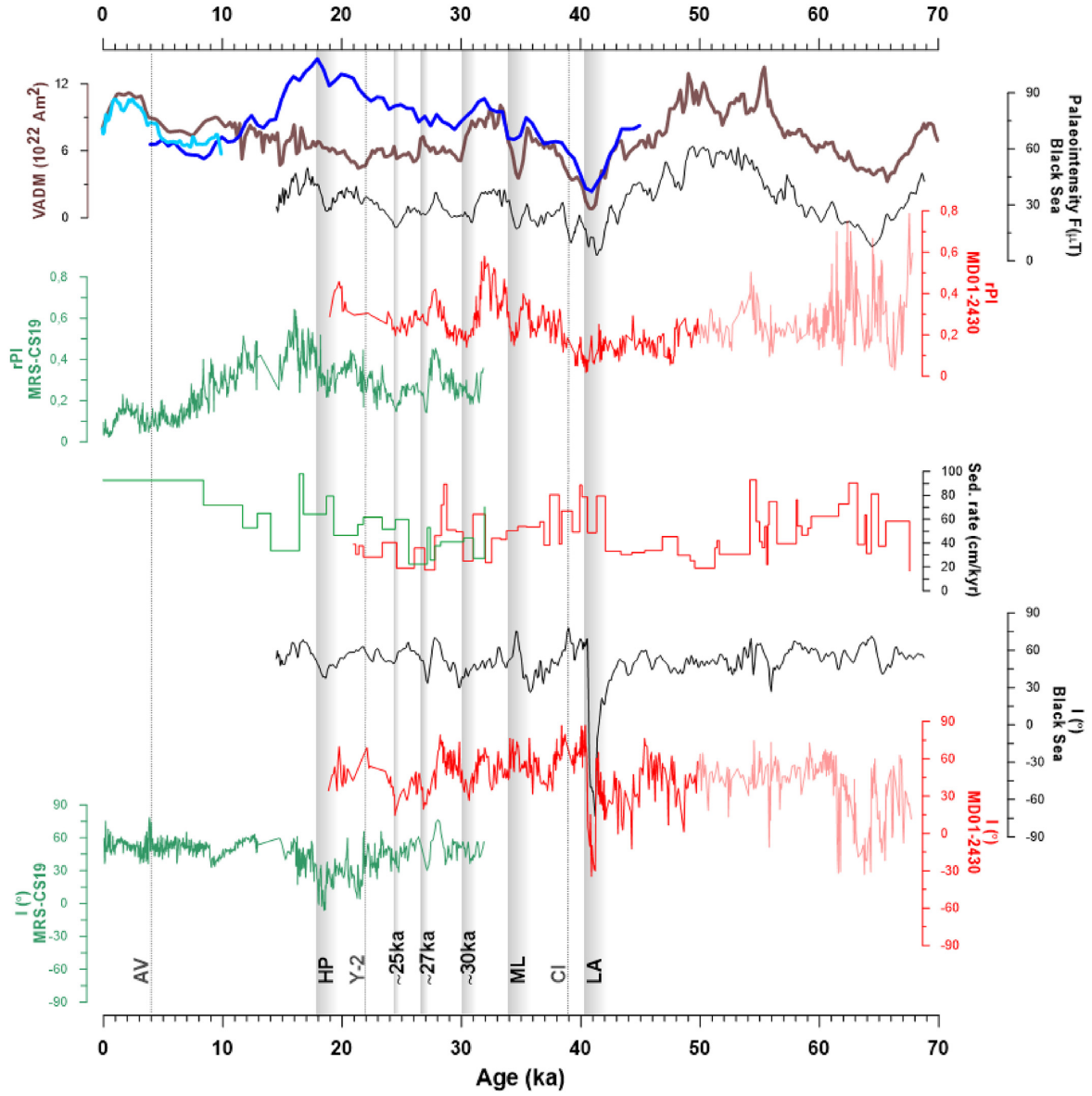

Figure 8. Palaeointensity and inclination records from cores MRS-CS19 (green) and MD01–2430 (red) over the last 70 ka. For comparison, the palaeomagnetic record from the Black Sea (black; Liu *et al.* subm.), the GLOPIS-75 record (brown; Laj *et al.* 2004), VADM stack (blue; Channell *et al.* 2018), and Holocene model (light blue; Korte *et al.* 2011) are also shown. Light red line shows unreliable RPI record of core MD01–2430. Vertical grey bars denote magnetic field excursions, LA (Laschamps), ML (Mono Lake) and HP (Hilina Pali). The dotted vertical lines mark the stratigraphic positions of the Avellino (AV), Cape Riva (Y-2) and Campanian Ignimbrite tephra (CI/Y-5) in the studied cores.

can be degraded by disturbances and discontinuous sedimentation (Roberts 2008), post-depositional processes and smoothing of remanence directions (Roberts & Winklhofer 2004). Nevertheless, our results indicate that the Sea of Marmara sediments effectively record the geomagnetic excursions.

Çağatay *et al.* (2015) showed that in core MD01–2430, the homogenous mud of the upper lacustrine succession (3.8–17.15 mbsf) was deposited between 12.55 ± 0.35 and 42.57 ± 1.7 cal ka BP. The interval below, covering 59–42 ka BP period, includes common carbonate bands with high Ca contents that correspond to the Greenland Interstadials. These interstadials are also represented by high TOC and low U and K contents. Due to climatic oscillations, the lithology of this interval is not homogenous as much as the upper part of the lacustrine interval. Laschamps excursion at 41 ka is recorded in the upper homogenous lacustrine succession at 16.6 mbsf. Rock magnetic properties of core MD01–2430, including the magnetic mineralogy and magnetic grain size, around the depth of the Laschamps excursion are stable except for the Campanian tephra record at the depth of 15 m (Fig. 5). *S*-Ratio and κ_{ARM}/κ_{LF} profiles of core MD01–2430 show that the magnetic mineralogy in 4–17.15 mbsf interval of upper lacustrine unit is not affected by sedimentary processes whereas 17.15–28 mbsf interval show the effect of the climatically controlled carbonate precipitation, with relatively high SIRM/κ_{LF} values (Fig. 5). MDF(NRM) values in 8–17.15 mbsf interval are stable except for the Laschamps excursion. Similar rock magnetic properties are also found at the depths of the Mono Lake and Hilina Pali excursions records in our cores MD01–2430 and MRS-CS19. We also obtained high MAD values during the Laschamps excursion. Stoner & St-Onge (2007) showed that such high MAD values are often found during reversals and

excursions. High MAD values at the depth of Laschamps record is related to an excursion rather than to any sedimentalogical change in lower part of core MD01–2430 (Fig. 6). Also, the low field intensities during an excursion could have led to a lower degree of magnetic particle alignment in the ambient field, and thus to a less well-defined direction.

The Laschamps excursion was followed by several short excursional episodes (Fig. 8), which can be correlated to the Mono Lake (Laj & Channell 2007; Nowaczyk *et al.* 2012; Channell *et al.* ; 2020) and Hilina Pali (Liu *et al.* 2018, and references therein) excursions with low palaeointensities and low/partly negative inclinations at 34.5 and 18 ka, respectively. In the Sea of Marmara sediments, the Mono Lake excursion at 34.5 ka is expressed by low palaeointensities without any clear directional anomaly, and shows good coherency with the Black Sea and GLOPIS records and the VADM stack of Channell *et al.* (2010, Fig. 8). Another palaeointensity with low and shallow (partly negative) inclination is recorded after the Mono Lake excursion at 18 ka, coeval with the postulated Hilina Pali excursion (Fig. 8). This is consistent with an interval of shallow inclinations which are also recorded in SE Black Sea sediments and are coeval with the postulated Hilina Pali excursion (Liu *et al.* 2018, and references therein). Coe *et al.* (1978) was the first to record the Hilina Pali excursion in a lava flow from Kilauea Volcano, Hawaii, with an age of 17.86 ka. However, the Hilina Pali excursion with low palaeointensities and shallow inclinations may represent a pronounced secular variation feature (Liu *et al.* 2018).

Numerous plausible excursions records for the last 30 ka period have been reported in the literature. These include the Sterno–Etrusso excursion at ∼2.7 ka (Dergachev *et al.* 2004), the Gothenburg excursion at ∼12 ka (Morner *et al.* 1971; Morner 1977), the Lake Mungo excursion at ∼26 ka (Barbetti & McElhinny 1976), an unnamed excursion in Core MD01–2444 from the Iberian Margin at ∼13 ka (Channell *et al.* 2013), the Tianchi excursion at 10 ka (Channell *et al.* 2020) and the Rockall excursion at ∼26 ka (Channell *et al.* 2016a). However, most of these excursions are yet to be definitely confirmed and dated by absolute and realiable methods. Well dated and high quality palaeomagnetic record of cores MRS-CS19 and MD01–2430 dating back to 34 ka BP show rPI lows also at 15, 25, 27 and 30 ka, which could be related with the above excursions (Fig. 8). At these ages, we also found shallow inclination directions. Sedimentation rates at 15, 25, 27 and 30 ka average 33, 22, 39 and 44 cm kyr^{-1}, respectively (Fig. 8). Hence, the low rPI values at these intervals are not likely related to a low sedimentation rate. The low rPI values in the SoM are compatible with the records of GLOPIS-75 (Laj *et al.* 2004), Black Sea (Liu *et al.* 2018; Liu et al. subm.) and VADM stack of Channell *et al.* (2018; 2020), with especially the low rPI at 27 ka likely related to the Rockall excursion (Fig. 8). However, for a robust regional and global comparison, acquisition of further records from the new cores are required.

Holocene RPI record from MRS-CS19 shows lower values throughout the core and a different trend than the record of Holocene interval in GLOPIS-75 (Laj *et al.* 2004) and Holocene record of Korte *et al.* (2011), except for the late Holocene interval (1–5 ka, Fig. 8). The sedimentation rate in the Marmara core rises across the L-M transition from 30 cm kyr^{-1} for the late lacustrine period (16–12.6 ka BP) to 80 cm kyr^{-1} during the middle-late Holocene (8.5 ka-present, Fig. 8). Low rPI values during middle to early Holocene, with a slight increase during 3–1 ka BP, are likely to be due to the relatively high sedimentation rate, possibly associated with changes in magnetic mineralogy and grain size after the L–M transition. Magnetic mineralogy and grain size variation in marine Holocene part is not stable as much as lacustrine part of core MRS-CS19 because of the early diagenetic effects.

6 CONCLUSIONS

A detailed palaeomagnetic study of two sediment cores from the Sea of Marmara yields results of variable quality. By linking the Ca-record (XRF counts) from core MD01–2430 to Greenland interstadials and stadials, together with AMS ^{14}C datings and tephrochronology, we demonstrate that cores MD01–2430 MRS-CS19 represent a continuous sequence that reaches back to about 70 and 32 ka BP, with average sedimentation rates of ∼43 and 68 cm kyr^{-1}, respectively.

Diagenetic effects are common especially in core MD01–2430, including the Holocene marine unit and the latest L–M transition zone deposited since 14.7 ka as well as the laminated lacustrine interval accumulated during 70–50 ka interval that are not suitable for palaeomagnetic analyses, while the marine and L–M transition zone in core MRS CS-19 provide a robust palaeomagnetic record. Palaeomagnetic data integrated from cores MRS-CS-19 and MD01–2430 yield evidence for the presence of three geomagnetic excursions. The Laschamps excursion (41.0 ka) is documented by low relative palaeointensities, negative inclinations and westerly declinations, which do not represent recording of a full reversal, as also reported from nearby Black Sea sediments (Nowaczyk *et al.* 2012). The Mono Lake excursion (34.5 ka) is evidenced only by a pronounced relative palaeointensity minimum. Shallow, partly negative inclinations and low relative palaeointensities in the Sea of Marmara palaeomagnetic record at ∼18 ka BP are likely to be an expression of the Hilina Pali excursion. General agreement is found between amplitudinal variations in our relative palaeointensity record from the Sea of Marmara and other regional and global records, such as the rPI stack from the Black Sea and GLOPIS-75.

ACKNOWLEDGEMENTS

This study was supported by the Scientific and Technological Research Council of Turkey (TUBITAK 115Y773) and the Deutscher Akademischer Austauschdienst (DAAD Funding 57210259). We thank Pierre Henry for supporting work on core MRS-CS19 and Frank Bassinot for sampling of core MD01–2430 at CNRS, Gif-sur-Yvette. We thank Nurcan Kaya, Melda Küçükdemirci, Mümtaz Hisarlı, İdil Urla, Gülay İşgüder and the EMCOL group for technical and logistical help during core processing and sampling. The authors also thank Andrew Roberts and the anonymous reviewer for their constructive comments that improved the paper.

REFERENCES

Aksu, A.E., Hiscott, R.N., Kaminski, M.A., Mudie, P.J., Gillespie, H., Abrajano, T. & Yaşar, D., 2002. Last Glacial-Holocene palaeoceanography of the Black Sea and Marmara Sea: stable isotopic, foraminiferal and coccolith evidence, *Mar. Geol.,* **190,** 119–149.

Andersen, K.K. *et al.*, 2006. The Greenland Ice Core Chronology 2005, 15–42 ka. Part 1: constructing the time scale, *Quat. Sci. Rev.* **25,** 3246–3257.

Armijo, R., Meyer, B., Navarro, S., King, G.C.P. & Barka, A.A., 2002. Asymmetric slip partitioning in the Sea of Marmara pull-apart: a clue to propagation processes of the North Anatolian fault?, *Terra Nova,* **14,** 80–86.

Barbetti, M.F. & McElhinny, M.W., 1976. The Lake Mungo magnetic excursion, *Philos. Trans. R. Soc. Lond.,* **281,** 515–542.

Berner, R.A. 1980. *Early Diagenesis: A Theoretical Approach,* Princeton Univ. Press.

Beşiktepe, Ş.T., Sur, İ.H., Özsoy, E., Abdul Latif, M., Oğuz, T. & Ünlüata, Ü., 1994. The circulation and hydrography of the Marmara Sea, *Prog. Oceanogr.,* **34,** 285–334.

Bloemendal, J., King, J.W., Hall, F.R. & Doh, S.-J., 1992. Rock magnetism of late Neogene and Pleistocene deep-sea sediments: relationship to sediment source, diagenetic processes, and sediment lithology, *J. geophys. Res.* **97,** 4361–4375.

Bonhommet, N. & Babkine, J., 1967. Sur la présence d'aimantation inversée dans la Chaîne des Puys, *C. R. Acad. Sci. Paris,* **264,** 92–94.

Bonhommet, N. & Zähringer, J., 1969. Palaeomagnetism and potassium argon age determinations of the Laschamp geomagnetic polarity event, *Earth planet. Sci. Lett.,* **6,** 43–46.

Borowski, W.S., Paull, C.K. & Ussler, W. 1996. Marine pore water sulfate profiles indicate in situ methane flux from underlying gas hydrate, *Geology,* **24,** 655–658.

Brandt, U., Nowaczyk, N.R., Ramrath, A., Brauer, A., Mingram, J., Wulf, S. & Negendank, J.F.W. 1999. Palaeomagnetism of Holocene and Late Pleistocene sediments from Lago di Mezzano and Lago Grande di Monticchio (Italy)—Initial results, *Quat. Sci. Rev.,* **18,** 961–976.

Çağatay, M.N., Borowski, W.S. & Ternois, Y.G. 2001. Factors affecting the diagenesis of Quaternary sediments at ODP Leg 172 sites in western North Atlantic: evidence from pore water and sediment geochemistry, *Chem. Geol.,* **175,** 467–467.

Çağatay, M.N. & Uçarkuş, G., 2019. Morphotectonics of the Sea of Marmara: basins and highs on the North Anatolian continental transform plate boundary,in *Transform Plate Boundaries and Fracture Zones,* Chapter 16, pp. 397–415. Elsevier.

Çağatay, M.N., Wulf, S., Sancar, Ü., Özmaral, A., Vidal, L., Henry, P., Appelt, O. & Gasperinni, L., 2015. The tephra record from the Sea of Marmara for the last ca. 70 ka and its palaeoceanographic implications, *Mar. Geol.,* **361,** 96–110.

Çağatay, M.N., Özcan, M. & Güngör, E., 2004. Pore-water and sediment geochemistry in the Marmara Sea (Turkey): early diagenesis and diffusive fluxes, *Geochem.: Explor., Environ., Anal.,* **4**(3), 213–225.

Çağatay, M.N. *et al.*, 2009. Late Pleistocene–Holocene evolution of the northern shelf of the Sea of Marmara, *Mar. Geol.,* **265,** 87–100.

Çağatay, M.N. *et al.*, 2019. The Sea of Marmara during Marine Isotope Stages 5 and 6, *Quat. Sci. Rev.,* **220,** 124–141.

Canfield, D.E. 1989. Reactive iron in marine sediments. *Geochim. Cosmochim. Acta.,* **53,** 619–632.

Caricchi, C. *et al.*, 2019. A high-resolution geomagnetic relative paleointensity record from the Arctic Ocean deep-water gateway deposits during the last 60 ky, *Geochem. Geophys. Geosyst.,* **20,** 2355–2377.

Channell, J.E.T., 2006. Late Brunhes polarity excursions (Mono Lake, Laschamp, Iceland Basin and Pringle Falls) recorded at ODP Site 919 (Irminger Basin), *Earth planet. Sci. Lett.,* **244,** 378–393.

Channell, J.E.T., Harrison, R.J., Lascu, I., McCave, I.N., Hibbert, F.D. & Austin, W.E.N., 2016. Magnetic record of deglaciation using FORC-PCA, sortable-silt grain size, and magnetic excursion at 26 ka, from the Rockall Trough (NE Atlantic), *Geochem. Geophys. Geosyst.,* **17,** 1823–1841.

Channell, J.E.T., Hodell, D.A., Crowhurst, S.J., Skinner , L.C. & Muscheler, R., 2018. Relative paleointensity (RPI) in the latest Pleistocene (10-45 ka) and implications for deglacial atmospheric radiocarbon, **191,** 57–72.

Channell, J.E.T., Hodell, D.A. & Curtis, J.H., 2012. ODP Site 1063 (Bermuda Rise) revisited: oxygen isotopes, excursions and palaeointensity in the Brunhes Chron, *Geochem. Geophys. Geosyst.,* **13**(1), Q02001.

Channell, J.E.T., Hodell, D.A., Margari, V., Skinner, L.C., Tzedakis, P.C. & Kesler, M.S., 2013. Biogenic magnetite, detrital hematite, and relative paleointensity in sediments from the Southwest Iberian Margin, *Earth planet. Sci. Lett.* **376,** 99–109.

Channell, J.E.T., Hodell, D.A., Singer, B.S. & Xuan, C., 2010. Reconciling astrochronological and 40Ar/39Ar ages for the Matuyama-Brunhes boundary and late Matuyama Chron, *Geochem. Geophys. Geosyst.,* **11,** Q0AA12.

Channell, J.E.T., Singer, B.S. & Jicha, B.R., 2020. Timing of Quaternary geomagnetic reversals and excursions in volcanic and sedimentary archives. *Quat. Sci. Rev.,* **228,** 106114.

Channell, J.E.T., Vázquez Riveiros, N., Gottschalk, J., Waelbroeck, C. & Skinner, L.C. 2017. Age and duration of Laschamp and Iceland basin geomagnetic excursions in the south Atlantic Ocean, *Quat. Sci. Rev.,* **167,** 1–13,

Channell, J.E.T., Xuan, C. & Hodell, D.A., 2009. Stacking palaeointensity and oxygen isotope data for the last 1.5 Myrs (PISO 1500), *Earth planet. Sci. Lett.,* **283,** 14–23.

Chauvin, A., Duncan, R.A., Bonhommet, N. & Levi, S., 1989. Palaeointensity of the earth's magneticfield and K-Ar dating of the Louchadiere vol-canicflow (Central France). New evidence for the Laschamp excursion, *Geophys. Res. Lett.,* **16,** 1189–1192.

Chiggiato, J. *et al.*, 2012. Dynamics of the circulation in the Sea of Marmara: numerical modeling experiments and observations from the Turkish straits system experiment, *Ocean Dyn*., **62**(1), 139–159.

Coe, R.S., Grommé, S. & Mankinen, E.A., 1978. Geomagnetic palaeointensities from radiocarbondated lava flows on Hawaii and the question of the Pacific nondipole low, *J. geophys. Res.,* **83,** 1740–1756.

Croudace, W., Rindby, A. & Rothwell, R.G., 2006. TRAX: description and evaluation of a new multi-function X-ray core scanner, in *New Techniques in Sediment Core Analysis,* Vol. **267,** pp. 51–63, eds Rothwell, R.G., Geological Society, London Special.

Dansgaard, W. *et al.*, 1993. Evidence for general instability of past climate from a 250-kyr ice-core record, *Nature*. **364,** 218–220

Dergachev, V.A., Raspopov, O.M., van Geel, B. & Zaitseva, G.I., 2004. The "Sterno-Etrussia" geomagnetic excursion around 2700 BP and changes of solar activity, cosmic ray intensity, and climate. *Radiocarbon,* **46,** 661–681.

De Vivo, B., Rolandi, G., Gans, P.B., Calvert, A., Bohrson, W.A., Spera, F.J. & Belkin, H.E., 2001. New constraints on the pyroclastic eruptive history of the Campanian volcanic plain (Italy), *Mineral. Petrol.,* **73,** 47–65.

Drab, L., Carlut, J., Hubert-Ferrari, A., Martinez, P., LePoint, G. & El Ouahabi, M., 2015. Palaeomagnetic and geochemical record from cores from the Sea of Marmara, Turkey: age constraints and implications of sapropelic deposition on early diagenesis, *Mar. Geol.,* **360,** 40–54.

Druitt, T.H., Edwards, L., Mellors, R.M., Pyle, D.M., Sparks, R.S.J., Lanphere, M., Davies, M. & Barriero, B., 1999. *Santorini Volcano,* Geological Society, London.

EIE (Elektrik İşleri Etüd İdaresi Genel Müdürlüğü), 1993. *Sediment Data and Sediment Transport Amount for Surface Waters in Turkey*. Publication No. 93–59, 615 pp.

Eriksen, U., Friedrich, W.L., Buchardt, B., Tauber, H. & Thomson, M.S., 1990. *The Stronghyle Caldera: Geological, Palaeontological and Stable Isotope Evidence From Radiocarbon Dated Stromatolites from Santorini,* pp. 139–150, eds Hardy, D.A. , Keller, J. , Galanopoulos, V.P. , Flemming, N.C., & Druitt, T.H., Thera and the Agean World III.

Eriş, K., Ryan, W.B.F., Çağatay, M.N., Sancar, U., Lericolais, G., Menot, G. & Bard, E., 2008. Reply to Comment on "The timing and evolution of the post-glacial transgression across the Sea of Marmara shelf south of Istanbul" by Hiscott et al., *Mar. Geol.,* **248,** 228–236.

Eriş, K.K., Ryan, W.B.F., Çağatay, M.N., Sancar, U., Lericolais, G., Menot, G. & Bard, E., 2007. The timing and evolution of the post-glacial transgression across the Sea of Marmara shelf south of İstanbul, *Mar. Geol.,* **243,** 57–76.

Eriş, K.K., Çağatay, M.N., Akçer, S., Gasperini, L. & Mart, Y. 2011. Late glacial to Holocene sea-level changes in the Sea of Marmara: new evidence from high-resolution seismics and core studies, *Geo-Mar. Lett*., **31**: 1–18.

Fabbro, G.N., Druitt, T.H. & Scaillet, S. 2013. Evolution of the crustal magma plumbing system during the build-up to the 22-ka caldera-forming eruption of Santorini (Greece). *Bull Volc*., **75**(12), 767.

Fisher, R.V., Orsi, G., Ort, M. & Heiken, G. 1993. Mobility of a large-volume pyroclastic flow – emplacement of the Campanian ignimbrite, Italy, *J. Volc. Geotherm. Res.,* **56,** 205–220.

Fossing, H. & Jørgensen, B.B. 1990. Oxidation and reduction of radiolabelled inorganic sulfur compounds in an estuarine sediment, Kysinf Fjord, Denmark, *Geochim. Cosmochim. Acta.,* **54,** 2731–2742.

Froelich, P.N. *et al.*, 1979. Early oxidation of organic matter in pelagic sediments of the eastern equatorial Atlantic: suboxic diagenesis. *Geochim. Cosmochim. Acta.,* **49,** 2097–2107.

Giaccio, B., Hajdas, I., Isaia, R., Deino, A. & Nomade, S. 2017. High-precision 14C and 40Ar/39Ar dating of the Campanian Ignimbrite (Y-5) reconciles the time-scales of climatic-cultural processes at 40 ka, *Sci. Rep.,* **7 ,**

Gillot, P.Y., Labeyrie, J., Laj, C., Valladas, G., Guèrin, G., Poupeau, G. & Delibrias, G., 1979. Age of the Laschamp palaeomagnetic excursion revisited, *Earth planet. Sci. Lett.,* **42,** 444–450.

Guillou, H., Singer, B.S., Laj, C., Kissel, C., Scaillet, S. & Jicha, B.R., 2004. On the age of the Laschamp excursion, *Earth planet. Sci. Lett.,* **227,** 331–343.

Halbach, P., Holzbecher, E., Reichel, T. & Moche, R., 2004. Migration of the sulphate-methane reaction zone in marine sediments of the Sea of Marmara–can this mechanism be tectonically induced? *Chem. Geol.,* **205,** 73–82.

Hammer, C.U., Clausen, H.B., Friedrich, W.L. & Tauber, H. 1987. The Minoan eruption of Santorini in Greece dated to 1645 BC?, *Nature,* **328,** 517–519

Horng, C.S., Roberts, A.P. & Liang, W.T., 2003, A 2.14-Myr astronomically tuned record of relative geomagnetic palaeointensity from the western Philippine Sea, *J. geophys. Res.,* **108**(B1), 2059.

Just, J., Sagnotti, L., Nowaczyk, N.R., Francke, A. & Wagner, B., 2019. Recordings of fast paleomagnetic reversals in a 1.2 ma greigite-rich sediment archive from lake ohrid, balkans. *J. geophys. Res.,* **124,** 12 445–12 464.

Kirschvink, J.L., 1980. The least-squares line and plane and the analysis of palaeomagnetic data, *Geophys. J. Int.,* **62,** 699–718.

Korte, M., Constable, C., Donadini, F. & Holme, R., 2011. Reconstructing the Holocene geomagnetic field, *Earth planet. Sci. Lett.,* **312,** 497–505.

Kotilainen, A., Saarinen, T. & Winterhalter, B., 2000, High-resolution palaeomagnetic dating of sediments deposited in the central Baltic Sea during the last 3000 years, *Mar. Geol.,* **166**(1), 51–64.

Kovacheva, M., Jordanova, N. & Karloukovski, V., 1998. Geomagnetic field variations as determined from Bulgarian archaeomagnetic data. Part II: the last 8000 years, *Surv. Geophys.,* **19,** 413–460

Laj, C. & Channell, J.E.T., 2007. Geomagnetic excursions , in *Treatise on Geophysics, Geomagnetism*, Vol. 5, pp. 373-416, eds Schubert G., et al., Elsevier, B.V.

Laj, C. & Channell, J.E.T., 2015. *Geomagnetic excursions*, in *Treatise on Geophysics,* 2nd edn., Vol. **5,** pp. 343–363, ed. Schubert, G., Elsevier.

Laj, C., Kissel, C. & Beer, J., 2004. High resolution global palaeointensity stack since 75 kyrs (GLOPIS-75) calibrated to absolute values , in *Timescales of the Palaeomagnetic Field,* Vol. **145,** pp. 225–265, eds Channell, J.E.T. , Kent, D.V., Lowrie, W. & , Meert, J.G., AGU Geophys. Monogr.

Laj, C., Kissel, C., Mazaud, A., Channell, J.E.T. & Beer, J., 2000. North Atlantic palaeointensity stack since 75 ka (NAPIS-75) and the duration of the Laschamp event, *Philos. Trans. R. Soc. Ser.,* **358,** 1009–1025

Laj, C., Kissel, C. & Roberts, A.P. 2006. Geomagnetic field behavior during the Iceland Basin and Laschamp geomagnetic excursions: a simple transitional field geometry?, *Geochem., Geophys. Geosyst.,* **7**(3),.

Langereis, C.G., Dekkers, M.J., de lange, G.J., Paterne, M. & van Santvoort, P.J.M. 1997. Magnetostratigraphy and astronomical calibration of the last 1.1 Myr from an eastern Mediterranean piston core and dating of short events in the Brunhes, *Geophys. J. Int.,* **129,** 75–94.

Le Pichon, X., Chamot-Rooke, N., Rangin, C. & Şengör, A.M.C., 2003. The North Anatolian fault in the Sea of Marmara, *J. geophys. Res.,* **108**(B4), 2179.

Levi, S. & Banerjee, S.K., 1976. On the possibility of obtaining relative paleointensities from lake sediments, *Earth planet. Sci. Lett.,* **29,** 219–226.

Li, G., Xia, D., Appel, E., Wang, Y., Jia, J. & Yang, X., 2018. A palaeomagnetic record in loess–palaeosol sequences since late Pleistocene in the arid Central Asia, *Earth Planets Space,* **70**(1), 44.

Liu, J., Nowaczyk, N., Frank, U. & Arz, H. 2019. Geomagnetic palaeosecular variation record spanning from 40 to 20 ka - implications for the Mono Lake excursion from Black Sea sediments. *Earth planet. Sci. Lett.,* **509,** 114–124.

Liu, J., Nowaczyk, N.R., Frank, U. & Arz, H.W., 2018. A 20–15 ka high-resolution palaeomagnetic secular variation record from Black Sea sediments – no evidence for the 'Hilina Pali excursion'?, *Earth planet. Sci. Lett.,* **492,** 174–185.

Liu, J., Nowaczyk, N.R., Panovska, S., Korte, M. & Arz, H. . The Norwegian-Greenland Sea, the Laschamps and the Mono Lake excursions recorded in a Black Sea sedimentary sequence spanning from 68.9 to 14.5 ka, *J. Geophys. Res.,* submitted.

Lund, S., Stoner, J.S., Channell, J.E.T. & Acton, G., 2006. A summary of Brunhes palaeomagnetic field variability recorded in Ocean Drilling Program cores, *Phys. Earth planet. Inter.,* **156,** 194–204.

Lund, S. 1996. A comparison of Holocene palaeomagnetic secular variation records from North America, *J. geophys. Res.,* **101,** 8007–8024.

Lund, S.P., Acton, G., Clement, B., Hastedt, M., Okada, M. & Williams, T. ODP Leg 172 Scientific Party, 1998. Geomagnetic field excursions occurred often during the last million years. *EOS, Trans. Am. Geophys. Un.,* **79**(14), 178–179.

Lund, S.P., Schwartz, M., Keigwin, L. & Johnson, T., 2005. Deep-sea sediment records of the Laschamp geomagnetic field excursion (∼41,000 calendar years before present), *J. geophys. Res.,* **110,** B04101.

Makaroğlu, O., 2011. *Van Gölü sedimanlarının çevre manyetizması ve palaeomanyetik kayıtları, PhD Thesis*. İstanbul Üniversitesi. Fen Bilimleri Enstitüsü.

McHugh, C.M.G., Gurung, D., Giosan, L., Ryan, W.B.F., Mart, Y., Sancar, U., Burckle, L. & Çağatay, M.N., 2008. The last reconnection of the Marmara Sea (Turkey) to the World Ocean: a palaeoceanographic and palaeoclimatic perspective, *Mar. Geol.,* **255,** 64–82.

Morner, N.A., 1977. The Gothenburg magnetic excursion, *Quat. Res.* **7,** 413–427.

Morner, N.A., Lanser, J.P. & Hospers, J., 1971. Late Weichselian palaeomagnetic reversal, *Nat. Phys. Sci.,* **234,** 173–174.

Morse, J.W. & Mackenzie, F.T. 1990. *Geochemistry of Sedimentary Carbonates. Developments in Sedimentology,* 48. Elsevier.

Muller, P.J. & Suess, E., 1979. Productivity, sedimentation rate, and organic matter in the oceans, *Deep-Sea Res.,* **26A,** 1347–1362.

NGRIP (North Greenland Ice Core Project) members, 2004. High resolution record of Northern hemisphere climate extending into the last interglacial period, *Nature,* **431,** 147–151

Nowaczyk, N.R., Antonow, M., Knies, J. & Spielhagen, R.F., 2003. Further rock magnetic and chronostratigraphic results on reversal excursions during the last 50 ka as derived from northern high latitudes and discrepancies in precise AMS14C dating, *Geophys. J. Int.,* **155,** 1065–1080.

Nowaczyk, N.R., Arz, H.W., Frank, U., Kind, J. & Plessen, B., 2012. Dynamics of the Laschamp geomagnetic excursion from Black Sea sediments, *Earth planet. Sci. Lett.,* **351–352,** 54–69.

Nowaczyk, N.R., Frank, U., Kind, J. & Arz, H.W., 2013. A high-resolution palaeointensity stack of the past 14 to 68 ka from Black Sea sediments, *Earth planet. Sci. Lett.,* **384,** 1–16.

Nowaczyk, N.R., Jiabo, L., Frank, U. & Arz, W.H., 2018, A high-resolution palaeosecular variation record from Black Sea sediments indicating fast directional changes associated with low field intensities during marine isotope stage (MIS) 4, *Earth planet. Sci. Lett.,* **484,** 15–29.

Nowaczyk, N.R. *et al.*, 2002. Magnetostratigraphic results from impact crater Lake El'gygytgyn, northeastern Siberia: a 300 kyr long high-resolution terrestrial palaeoclimatic record from the Arctic, *Geophys. J. Int.,* **150,** 109–126.

Okay, A.İ., Kaşlılar-Özcan, A., İmren, C., Boztepe-Güney, A., Demirbağ, E. & Kuşcu, İ., 2000. Active faults and evolving strike-slip basins in the Marmara Sea, northwest Turkey: a multichannel seismic reflection study, *Tectonophysics,* **321,** 189–218.

Okay, N. & Ergün, B., 2005. Source of the basinal sediments in the Marmara Sea investigatedusing heavy minerals in the modern beach sands, *Mar. Geol.,* **216,** 1–15.

Panovska, S., Korte, M. & Constable, C.G., 2019. One hundred thousand years of geomagnetic field evolution, *Rev. Geophys.,* **57,** 1289–1337.

Pichler, H. & Friedrich, W., 1976. Radiocarbon dates of Santorini volcanics. *Nature* **262,** 373–374

Plenier, G., Valet, J.-P., Guérin, G., Lefèvre, J.-C., LeGoff, M. & Carter-Stiglitz, B., 2007. Origin and age of the directions recorded during the Laschamp event in the Chaîne des Puys, *Earth planet. Sci. Lett.,* **259,** 414–443.

Ponte, J.M., Font, E., Veiga-Pires, C. & Hillaire-Marcel, C. 2018. Speleothems as magnetic archives: Paleosecular variation and a relative paleointensity record from a Portuguese speleothem, *Geochem. Geophys. Geosyst.,* **19**(9), 2962–2972.

Raiswell, R. & Berner, R.A. 1985. Pyrite formation in euxinic and semi-euxinic sediments, *Am. J. Sci.,* **285,** 710–724

Rasmussen, S.O., *et al.*, 2006. *A new Greenland ice core chronology for the last glacial termination,* **111,** D06102.

Reimer, P.J. *et al.*, 2013. IntCal13 and Marine13 radiocarbon age calibration curves, 0–50,000 years cal BP, *Radiocarbon,* **55,** 1869–1887.

Reynolds, R.L., Tuttle, M.L., Rice, C.A., Fishman, N.S., Karachewski, J.A. & Sherman, D.M., 1994. Magnetization and geochemistry of greigite-bearing Cretaceous strata, North Slope basin, Alaska, *Am. J. Sci,* **294,** 485–528.

Ricci, J., Carlut, J. & Valet, J.P., 2018. Paleosecular variation recorded by Quaternary lava flows from Guadeloupe Island, *Sci. Rep.,* **8,** 10147.

Roberts, A.P., 2008. Geomagnetic excursions: knowns and unknowns, *Geophys. Res. Lett.,* **35,** 17,307.

Roberts, A.P., 2015. Magnetic mineral diagenesis, *Earth Sci. Rev.,* **151,** 1–47.

Roberts, A.P. & Turner, G.M., 1993. Diagenetic formation of ferrimagnetic iron sulphides minerals in rapidly deposited marine sediments, South Island, New Zealand, *Earth planet. Sci. Lett.,* **115,** 257–273.

Roberts, A.P. & Winklhofer, M., 2004. Why are geomagnetic excursions not always recorded in sediments? Constraints from post-depositional remanent magnetization lock-in modelling, *Earth planet. Sci. Lett.,* **227,** 345–359.

Roeser, P.A. *et al.*, 2012. Lithostratigraphic and geochronological framework for the palaeoenvironmental reconstruction of the last 36 ka cal BP from a sediment record from Lake Iznik (NW Turkey), *Quat. Int.,* **274,** 73–87.

Ron, H., Nowaczyk, N.R., Frank, U., Schwab, M.J., Naumann, R., Striewski, B. & Agnon, A., 2007. Greigite detected as dominating remanence carrier in Late Pleisto- cene sediments, Lisan Formation, from Lake Kinneret (Sea of Gallilee, Israel), *Geophys. J. Int.,* **170,** 117–131.

Roperch, P., Bonhommet, N. & Levi, S., 1988. Palaeointensity of the Earth's magnetic field during the Laschamp excursion and its geomagnetic implications, *Earth planet. Sci. Lett.,* **88,** 209–219.

Sagnotti, L., Macri, P., Camerlenghi, A. & Rebesco, M., 2001. Environmental magnetism of Antarctic Late Pleistocene sediments and interhemispheric correlation of climatic events, *Earth planet. Sci. Lett.,* **191,** 65–80.

Sagnotti, L., Macri, P. & Lucchi, R.G., 2016. Geomagnetic palaeosecular variation around 15 ka ago from NW Barents Sea cores (south of Svalbard), *Geophys. J. Int.,* **204**(2), 785–797.

Schulz, D.H. 2000. Quantification of early diagenesis: dissolved constituents in marine pore water, in *Marine Geochemistry*, pp. 85–128, eds Schulz H.D., Zabel M., Springer.

Şengör, A.M.C., Grall, C., İmren, C., Le Pichon, X., Görür, N., Henry, P., Karabulut, H. & Siyako, M., 2014. The geometry of the North Anatolian transform fault in the Sea of Marmara and its temporal evolution: implications for the development of intracontinental transform faults, *Can. J. Earth Sci.,* **51,** 222–242.

Şengör, A.M.C., Tüysüz, O., İmren, C., Sakınç, M., Eyidoğan, H., Görür, N., Le Pichon, X. & Rangin, C., 2005. The North Anatolian fault. a new look. Annu. Rev. *Earth Planet. Sci.,* **33,** 37–112.

Sevink, J., van Bergen, M.J., van der Plicht, J., Feiken, H., Anastasia, C. & Huizinga, A., 2011. Robust date for the Bronze Age Avellino eruption (somma-Vesuvius) 3945 ± 10 cal BP (1995 ± 10 cal BC), *Quat. Sci. Rev.,* **30,** 1035–1046.

Snowball, I. & Thompson, R., 1990. A stable chemical remanence in Holocene sediments, *J. geophys. Res.,* **95,** 4471–4479.

Snowball, I.F., 1991. Magnetic hysteresis properties of greigite (Fe3S4) and a new occurrence in Holocene sediments from Swedish Lappland, *Phys. Earth planet. Inter.,* **68,** 32–40.

Stoner, J.S., Channell, J.E.T., Hodell, D.A. & Charles, C.D., 2003. A 580 kyr palaeomagnetic record from the sub-Antarctic South Atlantic (ODP Site 1089), *J. geophys. Res.,* **108**(B5), 2244

Stoner, J.S., Jennings, A., Kristjansdottir, G.B., Dunhill, G., Andrews, J.T. & Hardardottir, J., 2007. A palaeomagnetic approach toward refining Holocene radiocarbon based chronologies: palaeoceanographic records from North Iceland (MD99-2269) and East Greenland (MD99-2322) margins, *Palaeoceanography,* **22,** 1–23

Stoner, J.S., Laj, C., Channell, J.E.T. & Kissel, C., 2002. South Atlantic and North Atlantic geomagnetic palaeointensity stacks (0–80 ka): implications for inter-hemispheric correlation, *Quatern. Sci. Rev.,* **21,** 1141–1151

Stoner, J.S. & St-Onge, G., 2007. Magnetic stratigraphy: reversals, excursions, palaeointensity and secular variation, *Dev. Mar. Geol.,* **1,** 99–138.

Svensson, A. *et al.*, 2006. The Greenland Ice Core Project 2006, 15–42 ka. Part 2: comparison to other records, *Quat. Sci. Rev.,* **25,** 3258–3267.

Svensson, A. *et al.*, 2008. 60 000 year Greenland stratigraphic ice core chronology, *Clim. Past,* **4,** 47–57.

Tauxe, L., 1993. Sedimentary records of relative paleointensity of the geomagnetic field: theory and practice, *Rev. Geophys.,* **31,** 319–354.

Thompson, R. & Turner, G.M., 1979. British geomagnetic master curves 10,000-0 yr B.P. for dating European, *Geophys. Res. Lett.,* **6-4,** 249–252.

Thomson, J., Croudace, I.W. & Rothwell, R.G. 2006. A geochemical application of the ITRAX scanner to a sediment core containing eastern Mediterranean sapropel units, in *New Techniques in Sediment Core Analysis,* Vol. **267,** pp. 65–77, ed. Rothwell, R.G., Geological Society of London.

Thouveny, N. *et al.*, 1994. Climate variations in Europe over the past 140 kyr deduced from rock magnetism, *Nature,* **371,** 503–506.

Tolun, L., Çağatay, M.N. & Carrigan, W.J., 2002. Organic geochemistry and origin of Late Glacial-Holocene sapropelic layers and associated sediments in Marmara Sea, *Mar. Geol.,* **190,** 163–174.

Tric, E., Valet, J.P., Tucholka, P., Paterne, M., Labeyrie, L., Guichard, F., Tauxe, L. & Fontugne, M. 1992. Paleointensity of the geomagnetic-field during the last 80,000 years, *J. geophys. Res.,* **97,** 9337–9351

Tryon, M.D. *et al.*, 2010. Pore fluid chemistry of the North Anatolian Fault Zone in the Sea of Marmara: a diversity of sources and processes, *Geochem. Geophys. Geosyst.,* **11,** doi:10.1029/2010GC003177.

Ünlüata, Ü., Oğuz, T., Latif, M.A. & Özsoy, E., 1990. On the physical oceanography of the Turkish Straits, in *The Physical Oceanography of Sea Straits, NATO ASI Series,* ed. Pratt, L.J., pp. 25–60, Kluwer.

Valet, J.P., 2003. Time variations in geomagnetic intensity. *Rev. Geophys.* **41,** 1004.

Valsecchi, V., Sánchez-Goñi, M.F. & Londeix, L., 2012. Vegetation dynamics in the Northeastern Mediterranean region during the past 23 000 yr: insights from a new pollen record from the Sea of Marmara, *Clim. Past,* **8,** 1941–1956.

Verosub, K.L., 1977. Depositional and postdepositional processes in the magnetization of sediments, *Rev. Geophys. Space Phys.,* **15**(2), 129–143.

Verosub, K.L. & Banerjee, S. 1977. Geomagnetic excursions and their paleomagnetic record, *Rev. Geophys. Space Phys.,* **15**(2), 145–155.

Vidal, L., Menot, G., Joly, C., Bruneton, H., Rostek, F., Cagatay, M.N., Major, C. & Bard, E., 2010. Hydrology in the Sea of Marmara during the last 23 ka: implications for timing of Black Sea connections and sapropel deposition, *Palaeoceanography,* **25,** doi:10.1029/2009PA001735.

Vigliotti, L., Channell, J.E.T. & Stockhecke, M., 2014. Palaeomagnetism of Lake Van sediments: chronology and palaeoenvironment since 350 ka, *Quat. Sci. Rev.,* **104,** 18e29.

Wolff, E.W., Chappellaz, J., Blunier, T., Rasmussen, S.O. & Svensson, A., 2010. Millennial-scale variability during the last glacial: the ice core record, *Quat. Sci. Rev.,* **29,** 2828–2838.

Wulf, S., Kraml, M., Kuhn, T., Schwarz, M., Inthorn, M., Keller, J., Kuscu, I. & Halbach, P., 2002. Marine tephra from the Cape Riva eruption (22 ka) of Santorini in the Sea of Marmara, *Mar. Geol.,* **183,** 131–141.

Zheng, Y., Zheng, H., Deng, C. & Liu., Q., 2014. Holocene palaeomagnetic secular variation from East China Sea and a PSV stack of East Asia, *Phys. Earth planet. Inter.,* **236,** 69–78.

Zijderveld, J.D.A., 1967. AC demagnetization of rocks: analysis of results, in *Methods in Palaeomagnetism*, pp. 254–286, eds Runcorn S.K., Creer K.M., Collinson D.W., Elsevier.